Migration of the Antarctic Polar Front through the mid-Pleistocene transition: evidence and climatic implications.

A.E.S. Kemp[1][*], I. Grigorov[1,2], R.B. Pearce[1], A.C. Naveira Garabato[1]

[1]School of Ocean and Earth Science, National Oceanography Centre, Southampton, University of Southampton, Southampton, SO14 3ZH, UK

[2] Present address: Institut Universitaire Européen de la Mer, Technopole Brest-Iroise, Place Copernic, 29280 PLOUZANÉ, France.

[*] corresponding author
Professor Alan E S Kemp
School of Ocean and Earth Science
National Oceanography Centre Southampton
University of Southampton
European Way
Southampton
SO14 3ZH
UK

Tel 44 (0)2380592788
Fax 44 (0)2380593059
email aesk@noc.soton.ac.uk

Abstract

The Antarctic Polar Front is an important biogeochemical divider in the Southern Ocean. Laminated diatom mat deposits record episodes of massive flux of the diatom *Thalassiothrix antarctica* beneath the Antarctic Polar Front and provide a marker for tracking the migration of the Front through time. Ocean Drilling Program Sites 1091, 1093 and 1094 are the only deep piston cored record hitherto sampled from the sediments of the circumpolar biogenic opal belt. Mapping of diatom mat deposits between these sites indicates a glacial-interglacial front migration of up to 6 degrees of latitude in the early / mid Pleistocene. The mid Pleistocene transition marks a stepwise minimum 7 degree northward migration of the locus of the Polar Front sustained for about 450 kyr until an abrupt southward return to a locus similar to its modern position and further south than any mid-Pleistocene locus. This interval from a "900 ka event" that saw major cooling of the oceans and a $\delta^{13}C$ minimum through to the 424 ka Mid-Brunhes Event at Termination V is also seemingly characterised by 1) sustained decreased carbonate in the subtropical south Atlantic, 2) reduced strength of Antarctic deep meridional circulation, 3) lower interglacial temperatures and lower interglacial atmospheric CO_2 levels (by some 30 per mil) than those of the last 400 kyr, evidencing less complete deglaciation. This evidence is consistent with a prolonged period lasting 450 kyr of only partial ventilation of the deep ocean during interglacials and suggests that the mechanisms highlighted by recent hypotheses linking mid-latitude atmospheric conditions to the extent of deep ocean ventilation and carbon sequestration over glacial-interglacial cycles are likely in operation during the longer time scale characteristic of the Mid-Pleistocene Transition. The cooling that initiated the "900 ka event" may have been driven by minima in insolation amplitude related to eccentricity modulation of precession that also affected low latitude climates as marked by threshold changes in the African monsoon system. The major thresholds in earth system behaviour through the Mid-Pleistocene Transition were likely governed by an interplay of the 100 kyr and 400 kyr eccentricity modulation of precession.

Keywords: giant diatoms; *Thalassiothrix*; Antarctic Polar Front; mid-Pleistocene transition; mid-Brunhes event; insolation

1. Introduction

The mid-Pleistocene transition (MPT), the most profound secular reorganisation of the Earth system in recent geological time, involved a change from 40 kyr to 100 kyr paced glacial-interglacial cycles concurrent with a shift to greater glacial ice volumes (Berger and Jansen, 1994; Raymo et al., 1997) and coincided with the last global extinction in the deep sea (Hayward et al., 2007). The origins of the MPT are generally ascribed to the Earth system crossing a threshold in a cooling trend induced by a long-term decline in atmospheric CO_2 (Clark et al., 2006). One set of explanations for this threshold-crossing event involve the interaction between external forcing and internal, northern hemisphere, ice-sheet or sea-ice mediated feedbacks that promoted the 100 kyr cyclicity despite the relatively weaker eccentricity insolation forcing (Mudelsee and Schulz, 1997; Tziperman and Gildor, 2003; Clark et al., 2006). Alternative accounts point out that whereas atmospheric CO_2, Antarctic air temperatures, deep water temperature and tropical SSTs are in phase with eccentricity, ice volume lags these variables by several thousand years and so cannot be a driver (Shackleton, 2000; Medina-Elizalde and Lea, 2005). These studies implicate the response of the global carbon cycle to orbital forcing, leading Medina-Elizalde and Lea (2005) to speculate that the global carbon system was paced by obliquity changes during the early Pleistocene but that this response shifted to the eccentricity envelope of precession during the MPT.

Varied approaches to dating the MPT have led to a profusion of suggested ages for its inception, duration and conclusion. Foremost among dating methods stem from time series analysis based on recognition of an increase in amplitude and decrease in frequency of the benthic foraminiferal $\delta^{18}O$ signal, with the 100 kyr cycle first emerging at 1250 ka and becoming dominant between 700 – 600 ka (Mudelsee and Schulz, 1997; Mudelsee and Stattegger, 1997; Berger et al., 2005; Clark et al., 2006). However, a different perspective is provided by the analysis of critical changes in oceanic behaviour during the MPT. An interval of sustained low carbonate preservation in the South Atlantic that commenced with an extreme carbonate minimum at around 920 ka (during MIS 24) and persisted until about 530 ka (onset of MIS 13) is interpreted to represent reduced North Atlantic deep water (NADW) production and increased, corrosive, southern component water (SCW) influence

(Schmieder et al., 2000). From variations in the mean flow speed of the Deep Western Boundary Current (DWBC) off eastern New Zealand, Hall et al. (2001) similarly invoked a perturbation in global thermohaline circulation between about 870 ka (following MIS 22) to around 450 ka (during MIS 12) and regarded this interval as the MPT duration. The intervals around 900 ka and 450-500 ka also coincide with major perturbations in carbon cycle behaviour (Wang et al., 2004; Hoogakker et al., 2006), and ice cores demonstrate that interglacials prior to MIS 12, for the duration of the ice core record, had consistently lower atmospheric CO_2 levels than those since this time (Luthi et al., 2008; Hönisch et al., 2009). Extinctions of benthic foraminifers through the MPT further evidence significant changes in the ventilation as well as the temperature of intermediate and deep waters (Hayward et al., 2007), with the most significant extinctions in the South Atlantic occurring around MIS 20 (O'Neill et al., 2007).

While these apparently concurrent changes in ocean circulation and the carbon cycle on the MPT timescale currently lack a unifying framework, there is a convergence in the mechanisms proposed for such linkages on glacial-interglacial timescales involving increased isolation of deep waters from the atmosphere during glacials with relatively rapid ventilation of the deep Southern Ocean during deglaciation (Toggweiler et al., 2006; Watson and Naveira Garabato, 2006). In this hypothesis, during glacials, upwelling in the Southern Ocean is reduced in response to either a northward migration of the southern hemisphere mid-latitude westerlies or a change in air-sea buoyancy patterns, permitting respired CO_2 to accumulate in the deep ocean, but on deglaciation the reverse changes in atmospheric forcing promote upwelling and ventilation of the deep ocean. These theoretical and modelling-based scenarios appear to be supported by palaeo-observations (Anderson et al., 2009; Govin et al., 2009; Toggweiler, 2009).

Is it feasible to assess whether similar wind- and buoyancy-forced mechanisms operated over the longer timescale of the MPT? The westerlies drive the Antarctic Circumpolar Current (ACC), and the latitudes of the ACC jets associated with the major fronts of the Southern Ocean are closely related to wind forcing (Orsi et al., 1995). If palaeo-front indicators can be established, then it should be feasible to track the position of fronts and, by inference, the westerlies through time. Of the ACC

fronts, it is the Antarctic Polar Front (APF) that is the most biogeochemically significant, acting as an important nutrient divider with elevated levels of both silicate and nitrate to the south but only nitrate significantly present to the north (Pollard et al., 2002; Sarmiento et al., 2004). In addition to the deeper remineralisation of Si relative to N, it is the physical circulation at the front that promotes this nutrient imbalance (Naveira Garabato et al., 2002). Thus, north of the APF silicate is limiting (Nelson et al., 2001) with diatoms greatly subordinate to other phytoplankton and those present more lightly silicified and with less potential for sediment accumulation (Fenner et al., 1976; Hutchins et al., 2001). Beneath such waters carbonate sediments predominate. By contrast, south of the APF in the waters of the Antarctic zone, diatoms are the dominant primary producer and they appear to run a near monopoly on export accounting for 50-70% of the total global silica input to the deep oceans (Treguer et al., 1995; DeMaster, 2002; Cortese et al., 2004). This region, beneath and to the south of the APF contains much of the sedimentary legacy of the Southern Ocean's biological pump in a circumpolar opal belt that girdles Antarctica (Burckle, 1984; Burckle and Cirilli, 1987; Zielinski and Gersonde, 1997; Schlüter et al., 1998) and which has been active since 2.77 Ma (Cortese and Gersonde, 2008).

Evidence that the biogeochemical, micropalaeontological and sedimentological zones directly associated with the present Southern Ocean hydrography and location of the APF have moved significantly during glacial-interglacial cycles is not disputed (Charles et al., 1991; Diekmann and Kuhn, 2002; Gersonde et al., 2005; Flores and Sierro, 2007). However, the extent to which the APF itself may have migrated has been questioned. Some accounts suggest that, due to constraints of topography, the APF cannot have moved significantly from its present position (Moore et al., 2000). Indeed, a number of hypothetical scenarios have been put forward to account for the biogeochemical zones abandoning their relationship with the Southern Ocean hydrography at the last glacial maximum (LGM) (Anderson et al., 2002).

Whether or not the APF did move substantially presents significantly different scenarios both for reconstructing and modelling of glacial-interglacial changes, including mechanisms of CO_2 regulation. Indeed, frontal migration is tacitly assumed in some recent studies supporting the Toggweiler et al. (2006) mechanism, for example (Govin et al., 2009). Moreover, a new synthesis of evidence for migration of

the sub-tropical front supports linked APF migration (Bard and Rickaby, 2009). Hitherto, the debate over APF migration has been largely based on records from the circumpolar opal belt that span just one glacial cycle. Ocean Drilling Program Leg 177 was the first expedition to recover deep piston cores from the circumpolar opal belt, and continuous records from 3 sites (1091, 1093, 1094) represent a north-south transect spanning 6 degrees of latitude for the last 30 glacial cycles (Fig. 1). These sites include extensive laminated diatom mat deposits (Shipboard-Scientific-Party, 1999; Grigorov, 2004). A recent synthesis of oceanographic observations and paleo-data has highlighted the association between diatom mat accumulations and frontal zones (Kemp et al., 2006). Here we use the occurrence of laminated diatom mat deposits (LDM) as an independent indicator of frontal zone presence, and investigate movements of the position of the APF both on glacial-interglacial and on longer timescales associated with the major Pleistocene climatic changes, including the MPT and the Mid Brunhes Event. We then relate major changes in the location of the APF to other palaeoclimatic evidence to evaluate the possible driving mechanisms for mid Pleistocene climate change. Firstly we revisit the physical basis for frontal migration and briefly summarize evidence for the use of diatom mat deposits as frontal indicators.

Fig. 1 about here

2 Physical basis for APF migration

It has been proposed that the APF cannot have migrated significantly because of topographic constraints (Moore et al., 2000; Anderson et al., 2002). A closer look at the dynamics behind the formation of the ACC frontal jets leads us to dispel this proposition. The frontal jets arise from the competing interaction between two different processes acting on distinct spatial scales. First, large-scale forcing of the ocean by winds and air-sea-ice buoyancy exchanges drives an increase in the slope of the ACC density surfaces and, through geostrophy, accelerates a baroclinic current (Rintoul et al., 2001). A fundamental link between large-scale wind and buoyancy forcing and the latitudes of the ACC fronts is indicated by a broad coincidence between the locations of the major ACC frontal bands with enhanced meridional gradients in the wind-driven Ekman transport and the air-sea buoyancy flux [e.g.,

7

(Deacon, 1982; Rintoul and Sokolov, 2001)], and by significant co-variability between frontal positions and major modes of atmospheric variability on interannual (Dong et al., 2006; Sallée et al., 2008) and interdecadal (Böning et al., 2008) time scales. Second, the available potential energy contained in the tilt of the ACC density surfaces is released by baroclinic instability, which sheds a vigorous mesocale eddy field. Eddy evolution involves a gradual horizontal stretching that is ultimately arrested by the combined action of the Earth's rotation, sloping bottom topography and bottom friction cf Sinha and Richards (1999). This arrest of eddy growth leads to the formation of multiple, circumpolar fronts separated by a characteristic length scale of a few hundred kilometres. Thus, despite the role of topography in steering, splitting and focussing the ACC frontal jets (Hughes and Ash, 2001), only a few ridges and plateaux with prominent edges or passages constrain the latitudes of the jets decisively. Elsewhere, substantial shifts in the APF's characteristic latitude may conceivably be driven by a large-scale reorganization of the wind belts and seasonal sea ice cover, as hypothesized for stages during the Pleistocene (e.g. Gersonde et al., 2003).

This proposition is endorsed by coarse-resolution ocean models with realistic topography, which commonly predict that a meridional shift of the Southern Ocean wind belts will drive a corresponding shift of the ACC (Hall and Visbeck, 2002; Oke and England, 2004; Fyfe and Saenko, 2005; Saenko et al., 2005; Fyfe et al., 2007). Furthermore, eddy-permitting simulations of the ACC response to wind perturbation suggest that the coarse-resolution results likely simulate the control exerted by atmospheric forcing on frontal positions realistically. For example, (Treguier and Panetta, 1994) use an idealized channel model with eddy-permitting resolution to show that the meridional distribution of zonal wind stress firmly constrains the location and number of jets in an ACC-like flow, even in simulations where the jets are strongly steered by topography. Their findings are consistent with those of Sinha and Richards (1999), who demonstrate the relevance of the jet formation mechanism described above to the ACC in two different eddy-permitting ocean models. The same point is illustrated by (Hallberg and Gnanadesikan (2006), in whose eddy-permitting model the Polar Frontal Zone experiences a mean meridional shift of several degrees in response to interdecadal changes in wind stress.

3 Front palaeo-indicators

The evidence linking giant diatom ooze deposits and frontal zones has been summarized in a recent review (Kemp et al., 2006). Below, we briefly reiterate this evidence, specifically that linking laminated *Thalassiothrix* deposits (Fig. 2) and frontal zones, from the perspective of modern oceanographic observations, surface sediment surveys and ancient deposits.

Fig. 2 about here

3.1 Evidence from modern oceanographic surveys

In one of the most detailed surveys of the Polar Front in the Atlantic sector, concentrations of *Thalassiothrix* were observed north of the frontal jet (Klaas et al., 1997) in a position analogous to that of the equatorial Pacific "Great Front" *Rhizosolenia* concentrations (Yoder et al., 1994). These concentrations were inferred to originate from slow accumulation rather than a "bloom" (Tremblay et al., 2002). Syntheses of diatom abundance from sediment surface or core top samples show highest abundances for *Thalassiothrix* in the Polar Frontal Zone and northern Permanently Open Ocean Zone (Zielinski and Gersonde, 1997) consistent with deposition beneath the APF and associated ACC fronts.

3.2 Ecology of Thalassiothrix

In recent syntheses of diatom ecology (Kemp et al., 2000; Kemp et al., 2006) *Thalassiothrix* is characterised as a diatom adapted to stratified conditions whose water column abundance is primarily governed by processes of physical and / or physiologically-driven segregation rather than classical blooms. Observations of *T. antarctica* in deep chlorophyll maxima south of the APF or in the "Inter-Polar Front zone" (*sensu* Parslow et al. (2001)) are consistent with these characteristics (Kopczynska et al., 2001). Thus, within the waters south of the APF, *T. antarctica* is not dominant in surface waters, although it may be more important at depth. However, the net result of northward advection towards the APF at rates of 1 cm/s (Parslow et

al., 2001); (Strass et al., 2002) is to transport it to the frontal region with subsequent concentration (Tremblay et al., 2002) and mass flux.

3.3 Summary: Fronts and LDM formation

Water column concentrations of *Thalassiothrix* occur dominantly by physical and / or physiological mechanisms initiated by interaction with zones of frontal convergence (Kemp et al., 2006). Maximum occurrences in surface sediments support evidence for flux from such concentrations. Indeed, the frontal zone mechanism appears to be the main process capable of generating open ocean water column *Thalassiothrix* concentrations and massive flux. From ancient sediments it is evident that episodes of exceptionally high *Thalassiothrix* flux suppress benthic activity sufficiently to preserve successive individual diatom mat laminae, as well as intervening sediment, from disturbance (Kemp and Baldauf, 1993; King et al., 1995; Pike and Kemp, 1999) (Fig. 2). The degree of preservation of laminae in such deposits would appear to be proportional to the magnitude of *Thalassiothrix* flux. In turn, the magnitude of the *Thalassiothrix* flux at any location must relate to the geographic stability of the front over periods from seasonal through centennial. In addition, the absolute concentration of *Thalassiothrix* in the waters south of the APF may be enhanced by both increased stratification, to which it is well adapted, and nutrient concentration.

3.4 Other sedimentological, micropaleontological and geochemical evidence for Polar Front migration

The nature and sequence of changes in lithology and micropalaeontological composition of the relevant Sites (1091, 1093, 1094) also provide evidence for migration of the Polar Front. For example, at Site 1093, MIS 12 glacial sediments are dark, diatom-bearing, carbonate-free muds with abundant dropstones and containing diatom indicators of winter sea ice cover (Kunz-Pirrung et al., 2002). During the transition to MIS 11 (Termination V) this sediment is succeeded by diatom ooze containing LDM which is, in turn overlain by pale diatom-nannofossil ooze (Shipboard-Scientific-Party, 1999). Such southward shifts in carbonate deposition during interglacials have long been identified in Southern Ocean sediments and related to north-south migration of the APF during glacial-interglacial cycles (Howard

and Prell, 1992). Similarly N-S movement of microfossil types have also been used as evidence for frontal migration e.g. diatoms and radiolaria (Ciesielski and Weaver, 1983; Burckle, 1984; Morley, 1989; Gersonde et al., 2005) or calcareous nannofossils (Flores and Sierro, 2007). Systematic changes in Sr isotope tracers have also recently been used to infer meridional migration of the APF (Hemming et al., 2007). Important collateral support for APF migration is provided by evidence for migration of the Subtropical Front on glacial-interglacial time scales (Bard and Rickaby, 2009).

4. Methods and Material

4.1 Site locations and cores

ODP Leg 177 occupied a north-south transect of sites designed to encompass the major frontal systems of the South Atlantic (Gersonde and Hodell, 2002). The southernmost of these sites (1091, 1093, 1094) span the Polar Frontal Zone and permanently open ocean zone south of the present day location of the APF (Fig. 1). At each site, multiple holes were recovered in order to produce a continuous composite section. Inter-hole correlation was undertaken using shipboard Multi-Sensor Track (MST) data and % colour reflectance (650-750 nm) (Shipboard-Scientific-Party, 1999). The high compressive and tensile strength of the diatom mat deposits caused problems both with penetration and with pull-out of the piston corer particularly at Site 1093 and this militated against the recovery of deeper continuous sections. Fully continuous composite sections were constructed to 1.613 Ma (F O medium *Gephyrocapsa*; 1091), 1.057 Ma (Re-entry medium *Gephyrocapsa*; 1093) and 0.99 Ma (top Jaramillo; 1094) (Shipboard-Scientific-Party, 1999; Channell and Stoner, 2002; Flores and Marino, 2002).

4.2 Identification of Laminated Diatom Mat deposits
Laminated diatom mat deposits (LDM) were readily identified by the rough texture on core surfaces produced by tangled masses of the (up to) 4 mm long diatom *Thalassiothrix antarctica* (Fig. 2). The rough texture originates from the mats being effectively torn by the standard wire cutting method used for semi-consolidated sediment. The distribution of LDM was identified during shipboard visual core description (Kemp) and by subsequent re-examination of cores in the Bremen IODP

11

core repository (Kemp, Grigorov, Pearce). To complement and "ground truth" visual descriptions, smear slides were examined and electron microscopy was undertaken. Polished thin sections (PTS) of sediment samples were prepared by displacive fluid embedding using the method described in Dean et al. (1999) and the visual LDM logs were checked by backscatter electron imaging (BSEI) using a scanning electron microscope (SEM) (Fig. 3). Quantitative diatom counts were also undertaken from representative LDM intervals in conjunction with the SEM study. Diatom slides were prepared following the method outlined in Schrader (1974) and a minimum of 450 valves were identified to species level using the counting convention of Fenner (1991). Detailed diatom micropaleontology and BSEI results are reported elsewhere (Grigorov et al., 2002; *doi: 10.1594/PANGAEA.706805*), while representative BSE images of sediment lamina fabrics are shown in Fig. 3.

Fig. 3 about here

4.3 Age Model

A range of shipboard measurements and post-cruise results were pooled in order to place more accurately the occurrence of LDM with respect to glacial-interglacial transitions. Broad correlation and dating for the three sites was possible based on colour reflectance. Peak interglacial periods are identified by the increasing amount of pale carbonate ooze (high reflectance), while glacial sediments are dark-green to greenish gray (low reflectance) (Shipboard-Scientific-Party, 1999). The colour reflectance data agrees well with $\delta^{18}O_{N.pachyderma(s)}$ between marine isotope stage (MIS) 1-11 at Site 1094, (Kanfoush et al., 2002) and MIS 19-26 (sites 1091 and 1094, (Kleiven and Jansen, 2003) and has also been partially correlated between MIS 1-15 at Site 1093 (Kunz-Pirrung et al., 2002; Hodell et al., 2003a) and MIS 31 at Site 1094 (Scherer et al. 2008).

In order to date Site 1093 sediments to the same resolution as adjacent sites, the method discussed by Shaw (1964) and later by Edwards (1984) was adapted. For the last 1.5 My, Site 1094 was used as a master site against which the other two sites were compared. Kanfoush et al. (2002) demonstrated that magnetic susceptibility at Site 1094, is a very good proxy for ice-rafted debris (IRD) deposits, and where possible

(mainly between sites 1093 and 1094), magnetic susceptibility events at glacial onset and terminations were used to constrain the polynomial between the two sites. Additional data sets used included palaeomagnetic reversals (Channell and Stoner, 2002), $\delta^{18}O$ SPECMAP tie-points and MIS boundaries (Kanfoush et al., 2002), Gamma Ray Attenuation Porosity Evaluator (GRAPE) density (Shipboard-Scientific-Party, 1999) and biostratigraphic datums (Gersonde and Hodell, 2002). Based on the constrained polynomial of correlation between two sites, dated events were transferred (e.g. Jaramillo 0.99 Ma depth range can be determined in Site 1093 from Site 1094, based on the polynomial between the two sites; Fig. S1 -polynomial 1). The biostratigraphic data was not used to constrain the polynomials between Sites 1093 and 1094 (Fig. S1-a -polynomials 1 and 2), but they show good agreement in the depth-depth relationship between the two sites. Based on this agreement, biostratigraphy was used to establish depth-depth polynomials between sites when no other data was present, for example, between Sites 1094 and 1091, as magnetic susceptibility at Site1091 is noisy and unreliable, (Fig. S1-a -polynomials 3,4 and 6), and ultimately to provide absolute dates. Due to the lack of data, depth-depth polynomial 4 is oversimplified and the resultant age model for Site 1091, between 0 and 75 mcd (meters composite depth) is tenuous, although there are no LDM in this interval anyway.

Fig. 4 about here

Following the transfer of all dated events across all sites, depth-age data were fitted to a high order polynomial age model. Such a fit is statistically better than a linear relationship and also more realistic in terms of sedimentation rate changes (Fig. S1b,c,d). The low data density for the period 1.1-1.7 Ma, at Sites 1091 and 1093 (Fig. S1b,c), can potentially cause overfitting of the data when using a high order polynomial to better describe the rest of the data set. Such overfitting was minimized by using the biostratigraphic datums to constrain the depth-age polynomials. The resulting age models were used to date the occurrence of the LDM deposits.

5 Sedimentology, micropaleontology and distribution of laminated diatom mat deposits (LDM)

13

There are broadly three sediment compositional end-members within Sites 1091, 1093 and 1094. These are: 1) dark gray or greenish, often carbonate-free diatomaceous muds commonly with dropstones; 2) paler diatom ooze with variable quantities of *Thalassiothrix antarctica* diatom mats otherwise dominated by *Fragilariopsis kerguelensis*, with carbonate rare or absent, and 3) pale carbonate oozes with variable diatom content.

5.1 Micro-scale fabric analysis of laminated diatom mats (LDM)

LDM fabrics were categorised on the basis of the abundance and preservation of *T. antarctica* mats. Four categories were established based on visual core description complemented by optical microscopy and SEM analysis (Figs. 2, 3, 4). Generally, lamina preservation is directly related to the relative abundance of the pennate diatom *T. antarctica* as the entangled meshwork of *diatom* mats prevents bioturbation in the oxygenated waters of the deep ocean (King et al., 1995; Pike and Kemp, 1999); see Grigorov et al. (2002). Well-developed LDM are continuously laminated on a scale of decimeters to meters (e.g. MIS 27, Site 1093; Fig. 4; (Grigorov et al., 2002)). The preservation of the laminations is comparable to that observed in marginal oxygen minimum zone or silled basin settings (e.g. Dean et al., 2001). The high porosity associated with the sediment with greatest *T. antarctica* abundance produces a markedly darker image in BSEI. Intermittently laminated sediments exhibit a consistent alternation between laminated diatom oozes (LDO) and massive, non-laminated diatom oozes (MDO) on a cm scale (e.g. MIS 27, Site 1091; MIS 31,11/12 and 7, Site 1093; Fig. S1; (Grigorov et al., 2002)). Boundaries between massive and succeeding laminated sediment beds are abrupt, and signs of bioturbation originate within the massive intervals. Pellets, although rare, are most frequently observed in intermittently laminated beds, and tend to occur at the bedding interface between laminated and massive ooze intervals. Slightly or sparsely laminated and fragmented sediment fabric represents a significant part of the examined cores within which laminae are poorly preserved or comprise mat fragments only (Figs. 3, 4). Such deposits are most commonly observed throughout Site 1094, where the preservation of diatom mats is poor.

Fig. 4 about here

Micropalaeontological analysis involving conventional diatom counts demonstrates a general relationship between relative *T. antarctica* abundance and LDM fabric (Grigorov et al., 2002). In the intervals with the best preserved laminae (e.g. MIS 27 at Site 1093) *T. antarctica* abundance ranges from 15-25%, while in intervals of intermittent LDM preservation its abundance is in the range 2-10% (e.g. Termination V at Site 1093). In all cases the dominant diatom by conventional counting methods is *Fragilariopsis kerguelensis* (typically 50-80%). Conventional diatom counting of pennate diatoms relies on enumerating end poles. However, because a *T. antarctica* frustule may exceed 5 mm in length its proportional volumetric abundance is much greater than conventional diatom counting would indicate. Average length measurements taken from sediment trap samples are 1444µm for *T. antarctica* and 39µm for *F. kerguelensis* giving the former a 22 fold volume advantage (Grigorov, 2004). Thus, even for abundances as low as 5% *T. antarctica* still exceeds *F. kerguelensis* in volumetric significance.

5.2 Temporal and spatial distribution of LDM fabric

ODP Leg 177 recovered upper Pliocene sediments at sites 1091 and 1093, and lower Pleistocene sediments at Site 1094 (Fig. 4). Site 1091 has the best overall recovery of the three sites, with all of the material recovered using the advanced piston corer (APC). Use of the extended core barrel (XCB) at depth resulted in a rapid deterioration of recovery, for example in the Pliocene material from Site 1093. In terms of the occurrence through glacial-interglacial cycles, LDM are most abundant during transitions, especially terminations and in interglacials, but are less common in glacials. An account of the temporal distribution of described laminated fabric is divided into two intervals: (1) late Pliocene and early Pleistocene (1.7-1.0 Ma), (2) mid to late Pleistocene (1.0-0 Ma).

5.2.1 Pliocene and Early Pleistocene

There is good recovery at Site 1091 from 2.3 Ma with continuous recovery from 1.6 Ma. Fragmented mats, often preserved in burrow fills, occur intermittently through

the Pliocene and early Pleistocene at Site 1091. Starting around 1.5 Ma intermittently laminated fabrics are preserved with intervals of more contiguous lamina present from around 1.3Ma. At Site 1093 concentrations of *Thalassiothrix* are present in Pliocene sediments with thin horizons of LDM preserved in places, but recovery is so poor and discontinuous that it is not possible to formulate a coherent history of mat deposition over this time interval.

5.2.2 Mid to late Pleistocene

There is good core recovery in both sites 1094 and 1093 from around 1.3 Ma with continuous sections recovered from 1.15 Ma (1093) and 1 Ma (1094). In sediments younger than 1Ma, LDM are best represented during interglacial or transitional periods (Fig. 4) and of transitions, deglaciations more commonly contain the most abundant and best preserved LDM. Notable exceptions are during MIS 30 at Site 1091, where dating is well-constrained (Kleiven and Jansen, unpubl. data, 2002), and MIS 28 at Site 1093, where the age model is based on correlation with adjacent sites and is yet to be confirmed by δ^{18}O. The interval 780-520 ka is poorly dated in all sites. Although the age model is weakest here, the red color reflectance- δ^{18}O relationships suggests recognition of MIS optima is robust (Fig. 4). This is most evident at Site 1094 where the color contrast between glacial and interglacial sediment is highest (Fig. 4). Kanfoush et al. (2002) verified the red color reflectance- δ^{18}O relationship to be consistent for the last four glacial cycles.

No LDM occurs at Site 1091 in sediments younger than MIS 18 (750ka). There is a pervasive abundance of LDM within interglacials at Site 1093 between 1.3 and 1Ma. (It should be noted that although there was very poor recovery in the older Pleistocene at this site, this in itself was largely due to the inability to core LDM). Following a cessation at about 880 ka there is only one significant LDM occurrence at Site 1093 (at the MIS 15/14 transition) prior to a resumption of LDM deposition at Termination V (MIS 12/11 boundary) continuing to the Holocene (Fig. 4). At Site 1094, there are intermittent sparse occurrences between 1.3 Ma and 950 ka where an LDM at the start of MIS 25 marks the last occurrence until Termination V with deposition mainly of fragmented mat material occurring through to the Holocene. At sites 1093 and 1094, between MIS 23 and 25 respectively until MIS 12/11, foraminifer-bearing, diatom

oozes dominated by *Fragilariopsis kerguelensis* occur during interglacials and at some transitions in horizons that LDM might otherwise be expected to occupy. For the last four 100 kyr glacial cycles (MIS 11-1), Site 1093 remains the main locus of laminated sediment deposition, with significant intermittently laminated deposits observed during Termination V, Termination III and Termination II. At Site 1094, although mats are mainly fragmented, intermittently laminated intervals occur at Terminations V, IV III and II.

5.3 Sedimentation rates

During the late Pleistocene, periods with high sedimentation rates in sites 1093 and 1094 are associated with the occurrence of well-preserved LDM. The occurrence of intermittently laminated sediment fabric coincides with sedimentation rates consistently greater than 17cm ky^{-1}. The high dating density around 125 ka and 240 ka, shows that intermittent LDM have sedimentation rates of 37-40 cm ky^{-1}. A similar trend is observed in early Pleistocene sediments at Site 1091 where Kleiven and Jansen (unpublished data, 2002) have dated the 0.8-1 Mya period, with the best developed fabric associated with sedimentation rates of 20 cm ky^{-1} or higher. Where high resolution dating and correlation has been undertaken, for example across Termination II, a two- to four-fold increase in sedimentation rates is recorded in mat deposits reaching values of up to 70 cm ky^{-1} at Site 1094 (Bianchi and Gersonde, 2002). In an analysis based on the identification of possible annual lamina couplets, maximum sedimentation rates of between 57 cm ky^{-1} and 80 cm ky^{-1} are estimated which are consistent with the above conventionally estimated maximum rates (Grigorov et al., 2002). It is worth emphasizing that these values constitute the highest open ocean pelagic sedimentation rates ever recorded with comparable rates of 20-40 cm ky^{-1} documented only in analogous *Thalassiothrix* diatom mat deposits of Pliocene age in the eastern equatorial Pacific (Kemp et al., 2006). Silicon and carbon sediment mass accumulation rates range between 15 - 97 gSi/m^2/yr and 0.14 – 0.92 gC/m^2/yr (Kemp, et al., 2006).

6 Behaviour of the Antarctic Polar Front (APF) through the Pleistocene

Following from the analysis above, we are now in a position to summarize the evidence for migration of the Polar Front, both on glacial-interglacial timescales and on longer secular intervals through the Pleistocene (Fig. 5). Prior to about 1300 ka, the record is incomplete, especially at Site 1093, but the intermittently recovered continuous LDM here, compared with the predominantly fragmented mats found at 1091 suggest that the main locus of the front was around 50° South extending up to 47° South.

Fig. 5 about here

6.1 Frontal migration 1300 – 900 ka

The sparse LDM recovered at Site 1091 compared with more common intermittent or continuous LDM recovered at Site 1093 suggests a predominant location of the front, again around 50° South extending northward with a locus to around 47° South (the location of 1091). From the overall disposition of LDM in Sites 1091 and 1093 and a rare occurrence at Site 1094, a more detailed reconstruction may be attempted for the interval MIS 26 through 24, where LDM indicate an unusually large glacial – interglacial frontal migration. The APF apparently moved from a location between 47° and 50° South during the build up to MIS 26, and may have moved to a location further north at the glacial maximum, and then moved as far as 53° South during interglacial MIS 25. It then moved north to a location near Site 1091 in MIS 24, involving a glacial-interglacial movement of at least 6° of latitude. A glacial-interglacial APF migration of similar or slightly greater magnitude has been inferred from changes in calcareous nannofossil assemblages and sediment composition for the MIS 32-30 interval (Flores and Sierro, 2007).

6.2 Frontal migration 900 – 420 ka

Following the onset of MIS 22 at around 890 ka, LDM ceased at Site 1093 signifying the initiation of a major stepwise northward migration of the front from a locus spanning 47° - 50° South to a location at and to the north of 47° South marked by sparsely laminated and fragmented LDM that persist at Site 1091 (47° South) until ca.

740 ka (Fig. 5). Following 740 ka, a cessation of LDM deposition lasted until its abrupt return to sites 1093 and 1094 at ca. 420 ka with the exception of a minor sparse LDM at 1093. Possible explanations for the lack of LDM in this interval are: 1) The APF moved significantly to the north of all the present sites in stages, signifying a total northward migration of the locus of the APF greater than 7°. With LDM ceasing at 1093 after MIS 23, then ceasing at 1091 after MIS 18, this northward movement occurred in at least two steps with the interval of furthest northward penetration after 730 ka. 2) *Thalassiothrix* was not sufficiently abundant in the water column. If *Thalassiothrix* was not sufficiently abundant in the water column (due, for example to decreased nutrient supply) then despite frontal activity, there may not have been adequate flux to suppress benthic activity and form LDM. However, since high opal sedimentation rates are sustained at all sites during this period (Shipboard-Scientific-Party, 1999), a decreased nutrient supply does not seem likely. A further northward migration of the APF after 740 ka (option 1, above) appears most likely and would be consistent with other evidence including the stepped reduction in SST at Site 1090 from MIS 22 at 900 ka (Becquey and Gersonde, 2002; Martinez-Garcia et al., 2009).

6.3 Frontal migration 420 ka – present

The MIS 12/11 boundary (Termination V) at 424 ka, marks LDM evidence for the abrupt southward return of the APF to a locus including its present location at around 50° South and as far as 53° South, markedly further south than at any previous time in the mid-to-late Pleistocene. LDM sedimentation was sustained during interglacials and transitions (more commonly during deglaciation). Within the constraints of the age model there is some evidence for tracking of the APF between sites during successive glacial-interglacial cycles. For example, between MIS 6 and 4, LDM is prominent at 1093 during the 6-5 transition then ceases at 1093 but appears to the south, at 1094 during MIS 5 and then recurs at 1093 after cessation at 1094 during the transition to MIS 4. The lack of LDM at Site 1091 together with its newly sustained presence at 1094 demonstrates that the APF was now located further south than previously in the Pleistocene and strongly underpins evidence for reduced northward penetration of the APF following the end of the MPT. These APF movements are supported by the 650 kyr palaeotemperature record from Site 1094 of (Schneider-Mor

et al., 2005) that indicate markedly increased and more sustained interglacial summer sea surface temperatures after 430 kyr.

7 Relation of frontal migration to the Mid-Pleistocene Transition

7.1 The "900 ka event", northward frontal migration, and changes in deep circulation.

Within the period of considerable change that marks the MPT, one interval, centred broadly around 900 ka and termed the 900 ka event by Clark et al. (2006) stands out in records as a turning point (although as we will demonstrate in detail, it incorporates a series of "events" likely initiated by external insolation forcing that developed from around 940 ka). This corresponds to the interval of MIS 24 to 22 with intervening MIS 23 being markedly colder than previous odd numbered stages such that Clark et al. (2006) regard it as the first long glaciation of the Pleistocene. This also coincides with a global temperature minimum in SST records including the North Atlantic eastern tropical Atlantic, eastern equatorial Pacific, western equatorial Pacific (summarised in Clark et al., 2006) and marginal seas, e.g., South China Sea (Li et al., 2008).

7.1.1 Frontal migration: relation to surface circulation, SST and regional climate change
Beginning after MIS 23 at about 890 ka, LDM deposits indicate a stepwise northward migration of the APF. Contemporaneous northward penetration of colder waters that would be expected concurrently with frontal migration are evidenced by a series of South Atlantic SST studies. Alkenone and foraminiferal SST records from ODP Site 1090 (42°54'S) show an abrupt decrease in both glacial and interglacial temperatures following sustained low temperatures during the MIS 24-22 interval (Becquey and Gersonde, 2002; Martinez-Garcia et al., 2009). These reduced temperatures persisted, recovering only at MIS 11 (~ 420 ka around the Mid Brunhes Event (MBE)) and appear to covary with Antarctic air temperatures as recorded in the EPICA ice core over the past 800 ka (Jouzel et al., 2007; Martinez-Garcia et al., 2009). This decrease in SST reduced evaporation and led to an increase of aridity in Southern Africa as evidenced by a step change in clay mineralogy in detrital input to the Southern Ocean

(Site 1090) between 900 – 800 ka (Diekmann and Kuhn, 2002). Following cooling in the eastern tropical Atlantic during the MIS 24-22 interval, Schefuss et al. (2004) document a longer term warming trend to around 650 ka attributed to extreme northerly positions of South Atlantic fronts promoting intensified trade winds and enhanced return flow of warmer tropical waters from west to east (Schefuss et al., 2004). Low latitude cooling in the Atlantic may also have been promoted by the northward migrating fronts restricting Agulhas leakage of warm saline water from the Indian Ocean into the Atlantic (Becquey and Gersonde, 2002; Schefuss et al., 2004; Bard and Rickaby, 2009). Further evidence of such cooling is recorded by a $\delta^{18}O$ record from the planktonic foraminifer *Globorotalia inflata* from ODP Site 1082 at 21° South within the Benguela Coastal Current (BCC) showing significantly cooler SST in both glacials and interglacials from MIS 18 at around 760ka coinciding with the second northward movement of the APF and recovering only following MIS 12 (Jahn et al., 2003) (Fig. 5c).

7.1.2 Deep circulation changes

There is also evidence for a major change in deep circulation coinciding broadly with the 900 ka event with increased glacial inhibition of northern component waters in the deep North Atlantic (Venz and Hodell, 2002) and incursion of Southern Ocean deep waters into the North Atlantic, e.g. during MIS 21 (Kleiven et al., 2003). Furthermore, the sustained reduction in carbonate in the subtropical South Atlantic that developed around 920 ka (during MIS 24) and persisted until about 533 ka (onset of MIS 13), the so called "Mid-Pleistocene Interim State" is ascribed to reduced influence of NADW and increased importance of more nutrient and CO_2-rich and corrosive Southern Ocean deep waters (Schmieder et al., 2000). Such longer term reduction in NADW may have been associated with the suppression of the Agulhas leakage salt flux into the Atlantic by the northerly position of the fronts via a mechanism analogous to that proposed for NADW suppression on glacial-interglacial timescales (Peeters et al., 2004). These changes were also accompanied, during MIS 22, by a substantial decrease in the mean flow speed of the Deep Western Boundary Current (DWBC) flowing over Chatham Drift, revealed by analysis of sortable silt from that region (Hall et al., 2001) (Fig. 5b), and over the Chatham Rise as evidenced by magnetic grain size (Venuti et al., 2007) that persisted until MIS 12. The decrease in

the DWBC's strength is suggestive of a reduction in the rate of ventilation of the deep Pacific Ocean by dense Antarctic waters, and is consistent with a decline in AABW production and export during the MPT. The MPT is also marked by a series of extinctions of deep sea benthic foraminifera that have been related to decreasing glacial bottom water temperatures and reduced deep water ventilation (Hayward et al., 2007), with the most dramatic decline in abundance and diversity occurring during MIS 20 (O'Neill et al., 2007). Thus, the MPT period (ca. 900 - 430 ka) appears to have been characterized by a relatively sluggish renewal of the deep ocean's water masses compared to periods of several hundred kyr before or after.

7.2 The "mid-Brunhes event" (424 ka), Termination V, southward return of the APF and restoration of deep ventilation

During Termination V, LDM deposition abruptly returned to 1093 and commenced substantively for the first time at 1094 marking a southward return of the APF. Termination V is also marked by a step increase in Southern Ocean temperatures through glacial / interglacial cycles sustained for the last 400 ka (Martinez-Garcia et al., 2009). The episode of change through Termination V has been referred to as the "Mid-Brunhes Event" (MBE), and the originators of this term (Jansen et al., 1986) also documented evidence for a southward migration of the APF (Ciesielski and Weaver, 1983). The Benguela Current system also rapidly warmed during Termination V to reach a consistently higher interglacial and glacial temperature pattern persisting to the present (Jahn et al., 2003) (Fig. 5c). Furthermore,Termination V coincided with an increase in the strength of the northward limb of the deep Pacific circulation, for the first time attaining higher speeds than prior to the 900 ka event (Fig. 5b), possibly indicative of an intensification of AABW formation and export (Hall et al., 2001). This major reconfiguration of ocean circulation at the MBE occurred concurrently with a further increase in ice volume variation (Lisiecki and Raymo, 2005) (Fig. 5f). Compared with the last 400 ka, the pre – MBE, 900 – 424 ka period is generally marked by lower-amplitude glacial-interglacial cycles, significantly cooler interglacials but of longer relative duration, and lower interglacial CO_2 values (EPICA et al., 2004; Luthi et al., 2008).

The last phase of the MPT is also notable for the occurrence of *Ethmodiscus rex* giant diatom ooze deposits in cores located between 29° and 32° South in the subtropical South Atlantic within glacial stages MIS 14 (537 ka) and MIS 12 (432 ka) (Romero and Schmieder, 2006). The location of these deposits has been related to a possible extreme northerly position for the Subtropical Front (Gingele and Schmieder, 2001) while their timing has been related to a broader body of evidence for a widespread return to more humid conditions in low latitudes at this time with enhanced weathering and run-off delivering silica-enriched water as well as isotopically light carbon (Wang et al., 2004). An alternative but possibly complementary explanation connects the silica availability to an abrupt strengthening of the thermohaline circulation (Gingele and Schmieder, 2001); (Romero and Schmieder, 2006), a scenario supported by the link between deep ventilation and diatom productivity and flux during the most recent termination (Anderson et al., 2009). Significantly a sparse LDM occurs during MIS 14 at Site 1093 that may represent the same abortive deep ventilation and silica upwelling event possibly associated with a brief return of the APF.

From Termination V, for the last four 100 kyr glacial cycles, the APF has occupied its most southerly Pleistocene position and has undergone similar glacial-interglacial migrations. Therefore, although the 100,000 year cycles may have been established from around 640 ka, a step-change in the location of the APF, and an associated fundamental reorganisation of the Earth system (ocean circulation, temperature, CO_2, ice volume) did not occur until the amplitude of glacial-interglacial cycles increased to that characteristic of the last 400 kyr at the MBE.

7.3 The carbon cycle through the MPT

The "900 ka event" is also marked by a prominent minima in oceanic $\delta^{13}C$ values, with a 0.3 per mil decrease between 1 Ma and 900 ka attributed to a one-off addition of terrestrial carbon to the oceanic reservoir associated with increased aridity and a reduction in C biomass (Raymo et al., 1997; Venz and Hodell, 2002). In a subsequent study of trends in benthic $\delta^{13}C$ from smoothed (60 kyr filter) stacked records from a range of ocean basins Hoogakker et al. (2006) show a 0.35 per mil reduction between

1 Ma and 900 ka that they term the MPCF (Mid Pleistocene δ^{13}C fluctuation) (Fig. 5d). They then document a more gradual return to pre- 1 Ma values until 500 ka when there is a further rapid 0.3 per mil reduction with a rapid step to 420 kyr termed the LPCF (Late Pleistocene δ^{13}C fluctuation). Wang et al. (2004) relate both the MPT at 900 ka and the MBE at 424 ka to the preceding δ^{13}C maxima (Fig. 5d) (which they name δ^{13}Cmax-III and δ^{13}Cmax-II, respectively) and suggest that such changes in the carbon system can modify the response of the ice climate system to orbital forcing, although they did not propose a mechanism. Thus, both the stepped northward migration of the APF (900 ka event) and the abrupt southerly return at the MBE are preceded by δ^{13}C minima following 0.3 to 0.35 per mil decreases from corresponding δ^{13}C maxima (Fig. 5d).

8. Relation of frontal migration to the mid-latitude westerlies and the ocean carbon cycle

The above account of the association between the APF migration, changes in ocean circulation and climate, and the evolution of the carbon cycle may be interpreted in the context of recent model-based investigations of the relationship between the location of the mid-latitude westerlies and atmospheric CO_2 over glacial-interglacial cycles (Toggweiler et al., 2006). This builds on the "chemical divide" model of Toggweiler (1999) that identifies changes in deep ocean ventilation as a major player in causing glacial-interglacial atmospheric CO_2 variations, and which has garnered support from paleoceanographic studies of deep sea carbonate and δ^{13}C gradients (Hodell et al., 2003b) and marine radiocarbon evidence (Marchitto et al., 2007). In this hypothesis, warm interglacial climates have poleward-shifted westerlies that flush respired CO_2 out of the deep ocean (although the physical mechanism ultimately controlling deep ocean ventilation may be only indirectly related to the latitude of the westerlies, see Watson and Naveira Garabato (2006) for a discussion). Furthermore, cold glacials have equatorward-shifted westerlies that are associated with upwelling too far north to ventilate the deep ocean, causing the build up of respired CO_2 (Toggweiler et al., 2006). Thus, the key ingredient of this hypothesis is a plausible link between the latitude of the westerlies and the vertical horizon of ventilation in the ocean basins north of that latitude.

The impact of this link on atmospheric CO_2 variability over glacial-interglacial timescales is accentuated by a further apparent correspondence between the latitude of the westerlies and the rate of AABW production and export. As demonstrated by Hall et al. (2001), glacial periods are characterised by intensified northward export of dense Antarctic waters to the deep Pacific Ocean, and the reverse is true for interglacials. (We note, though, that seemingly contradictory evidence of weaker glacial bottom water flow in the Cape Basin is presented by Kuhn and Diekmann (2002), pointing to regional variability in the response of AABW circulation or to differences in proxy interpretation.) It has been argued (Watson and Naveira Garabato, 2006) that the increased glacial production of AABW was associated with an intensified seasonal cycle of Southern Ocean sea ice that also brought about a reduction in the rate of deep Southern Ocean upwelling. If so, this would have contributed to accumulating respired CO_2 in the ocean abyss, reinforcing the connection between the location of the mid-latitude westerlies and atmospheric CO_2. The direct evidence of reduced ventilation of the deep Southern Ocean from depleted $\delta^{13}C$ in benthic foraminifera (Hodell et al., 2003b) is further supported by the sediment evidence of Kuhn and Diekmann (2002).

The westerlies are the primary driver of the ACC system, however they are less constrained as regards meridional migration than the ACC, which ultimately must pass through Drake Passage and negotiate several major topographic obstacles. Nevertheless, we would expect a broad correspondence in the direction of meridional migration of the westerlies and the ACC fronts, with perhaps a few exceptions in the vicinity of the most prominent bathymetric obstructions, see for example Sallée et al. (2008) for a present-day example. During the MPT, interglacial CO_2 levels were some 30 per mil lower than those during and since MIS 11(Siegenthaler et al., 2005). This scenario fits with our inferred extreme northerly location of the APF because during this period, even in interglacials, the westerlies would not have been sufficiently far south to fully ventilate the deep ocean leading to the sustained reduction in carbonate in the South Atlantic sediments during the MPT (Schmieder et al., 2000) (Fig. 5). This is also consistent with recent model simulations that ascribe the lower interglacial CO_2 levels prior to Termination V to the thermohaline circulation

remaining in weaker "glacial" mode coupled with lower Southern Ocean SST (Kohler and Fischer, 2006).

Note, however, that the analogy between the mechanisms controlling atmospheric CO_2 over glacial-interglacial cycles and the MPT timescale breaks down in regard of the rate of AABW production and export. On the longer MPT timescale, a reduction in this rate is associated with a northward displacement of the westerlies, whereas the opposite relationship applies over glacial-interglacial periods throughout the available CO_2 record. This is symptomatic of the importance of distinct driving processes on the MPT timescale. The foremost of these may result from the surface water cooling that was widespread around the 900 ka event (see Figures 5, 6 and 13 of Clark et al. (2006)) especially that occurring at high southern latitudes (Martinez-Garcia et al., 2009). Such cooling in high-latitude surface waters is likely associated with a critical reduction in the density contrast between surface and deeper waters sufficient to inhibit sinking (Russell et al., 2006; de Boer et al., 2007). The evidence of reduced flow in the DWBC (Hall et al., 2001) suggests that such inhibition may have been a sustained feature of an interim state of deep ocean circulation through the MPT. Thus, surface temperatures in the subpolar seas surrounding Antarctica likely decreased (increased) in conjunction with the northward (southward) migration of the westerlies and the APF over both of the time scales under discussion here, as would be expected from a simple conceptualization of the westerlies-APF coupled system as a barrier to the import of heat from the subtropics. However, it is possible that a SST threshold may exist below which the temperature dependence of the AABW production rate reversed sign. The attainment of this threshold would have been promoted by the minimum in insolation leading to the 900 ka event (Figs 5,6). This led to colder surface waters and a weaker seasonal sea ice cycle, which would have prevented the surface waters from getting dense enough to form substantial AABW. The further insolation minima, driven by eccentricity modulation of precession, straddling 800 ka sustained this cooling as evidenced by the significantly cooler temperatures of the Benguela Coastal Current (BCC) at this time during both glacials and interglacials (Jahn et al., 2003) (Fig. 5). The sustained cooling of the BCC does not occur until the second and most extreme northward migration of the APF during MIS 18, and may have been further promoted by increased restriction of the warm Agulhas leakage such that the BCC became largely supplied by cooler high latitude Southern Ocean

waters. This cooling persisted until the southward return of the APF following MIS 12 (Fig. 5).

The abrupt southward return of the APF during Termination V coincides with the attainment of the higher interglacial atmospheric CO_2 values characteristic of the late Pleistocene and is consistent with the interglacial westerlies attaining a sufficiently southerly position to thoroughly ventilate the interglacial deep ocean. It therefore follows that if the "Mid Pleistocene Interim State" is considered to be the interval in which there was sustained inhibition of NADW and reduced ventilation of the deep ocean then its duration extended from 880 ka until 430 ka. Although ice core records of atmospheric CO_2 do not extend beyond 800 ka, recent atmospheric CO_2 reconstructions based on boron isotope records suggest that interglacial atmospheric CO_2 levels prior to 892 ka were similar to those of the last 420 ka (Hönisch et al., 2009), thus supporting this ca. 450 kyr duration for the period of reduced deep ocean ventilation.

The consequences of the deglacial ventilation hypothesis also provide further explanation for the occurrence of the most intense diatom mat sedimentation during deglaciations / terminations, in that silicic acid, abundant in Southern Ocean deep waters, would also be brought to the surface, following Anderson et al. (2009). This would then further enhance silica levels in Southern Ocean surface waters, already boosted by meltwater, fuelling diatom mat production.

9 Driving mechanisms for the 900 ka event and the MBE
We now revisit the origins of the MPT in relation to external orbital forcing. While there is no doubt that the MPT is associated with an underlying cooling trend, syntheses such as that presented above and that of Clark et al. (2006) point to more abrupt events that punctuate the overall transition. For example, if the beginning (900 ka event) and end (MBE) of the Mid Pleistocene Interim State evidently represent thresholds in Earth system behaviour, the question remains: how were they crossed?

Figs 6 and 7 about here

9.1 The 900 ka event

27

One obvious factor in the lead up to the 900 ka event is the change in external forcing involving a stepped decrease in the maximum insolation during precession minima at around 940 ka that was sustained for some three further cycles (Laskar et al., 2004) (Figs. 5, 6) and is related to 100 kyr eccentricity modulation of precession (Fig. 6 c, d). This may have been critical in allowing the maintained cooling through MIS 24 and 22 with subdued interglacial MIS 23, and would also have been an important driver of the widespread minima in SSTs at this time (e.g. (Clark et al., 2006); Fig. 5). Elsewhere in the Earth system the effect of this was marked, with reduced northward penetration of the African Monsoon leading to increased north African aridification evidenced by a step increase in dust flux to the Mediterranean after 940-930 ka (Larrasoana et al., 2003) and a lacuna in Mediterranean sapropel deposition following sapropel S'' at 955 ka (Lourens, 2004) (Fig. 6a, b). Following the Toggweiler et al. (2006) hypothesis, this insolation-led cooling drove a northward movement of the westerlies and associated frontal systems, that, in turn, caused reduced deep overturning and ventilation in the Southern Ocean. Meanwhile, the northward migrating frontal systems likely inhibited the Agulhas supply of warm saline Indian Ocean water to the South Atlantic (Sijp and England, 2008; Bard and Rickaby, 2009) and reduced deep convection in the North Atlantic (Fig. 7). Sustained ocean cooling through the MPT would have been promoted by the marked decrease in insolation amplitude related to 400 kyr eccentricity-modulation of precession around 800 ka and this would have promoted the second northward migration of the APF and Benguela Current cooling (Figs. 5,6). This 400 kyr period is known to have become dominant following 1 Ma (Crucifix et al., 2006) and has characterised earlier periods in the Cenozoic (Pälike et al., 2006). The widespread surface ocean cooling that also affected the eastern equatorial Pacific led to the onset of a modern Walker circulation that is associated with elevated moisture transport to high latitudes permitting the development of larger ice sheets and thus promoting the shift to the 100 kyr cycles (McClymont and Rosell-Mele, 2005).

9.2 The mid-Brunhes event.

The beginning of the MBE (about 424 ka) occurred after a major ice sheet expansion during MIS 12 and was followed by Termination V, which represented the largest

relative change in $\delta^{18}O$ and ice volume since the Miocene with sea levels rising from 20 m below those of the LGM (Rohling et al., 1998). The return of LDM during Termination V signifies southward return of the fronts while other hydrographic proxies, the sortable silt and magnetic grain size, indicate increasing DWBC flow from about 450 ka (Hall et al., 2001; Venuti et al., 2007) (Fig. 5). The hydrographic proxies are therefore consistent with the EPICA CO_2 record indicating an onset of deep ventilation towards the MIS 12/ 11 transition engineered by a strengthening of abyssal circulation. In contrast to this chronology (Schmieder et al., 2000) propose a MPT "terminal event" at ca. 530 ka represented by giant diatom deposits during MIS 14 (Romero and Schmieder, 2006). This coincides with a minor interval of LDM at site 1093 but given evidence of change at Termination V likely represents a brief, abortive attempt at system reorganisation. Intriguingly this coincides with an interval of reduced insolation amplitude driven by a 100 kyr minimum in the eccentricity envelope of precession. As to what caused the resumption of deep ventilation at Termination V, it may be that sustained low insolation maxima following 460 ka (Fig. 5g) (related to a 400 kyr eccentricity minimum) may have allowed the greater ice accumulation to build up during MIS 12 while the amplitude and rapidity of Termination V may have kick-started the reorganisation of deep ocean circulation.

9.3 Carbon cycle changes

What then was the role of the carbon cycle in these events? Both the 900 ka event and the MBE (and associated APF movements) occur at prominent minima in oceanic $\delta^{13}C$, which in turn follow similarly spaced oceanic $\delta^{13}C$ maxima (Fig. 5d). This sequence led Wang et al. (2003) to view major ice sheet growth at these times as a consequence of perturbations in carbon reservoirs and relate the spacing of such episodes to a longer term 500 kyr cyclicity in $\delta^{13}C$ records over the past 5 Myr (Wang et al., 2004).

On the basis of a 13 Myr Oligocene $\delta^{13}C$ record, Pälike et al. (2006) postulated that the Earth "breathes" in 400 kyr periods regulated by insolation forcing of biological productivity. For the MPT, however, it appears that insolation-forced changes in ocean circulation acted as a "pacemaker" for carbon cycle regulation and that both the

100 kyr and 400 kyr modulation or envelope of precession appear to have been critical drivers. The dynamics of the 900 ka event suggests that the 100 kyr cycle was the tipping force but that the 400 kyr cycle was important in sustaining and reinforcing the transition. The 500 kyr cyclicity in the C cycle over the last 5 Ma noted by Wang et al. (2004) and present in other records may simply correspond to this type of interplay between the 400 kyr and 100 kyr envelope of precession giving the near 500 kyr pacing between the 900 ka event and the MBE.

It may therefore be that the carbon cycle was merely responding to the insolation-driven changes described above. Hoogakker et al. (2006) point out that the cessation of Mediterranean sapropel deposition after 955 ka is concurrent with reduced carbon fluxes elsewhere (including the Sea of Japan and the South Atlantic) and they consider the 900 ka δ^{13}C minimum to result from a change in carbon burial and/ or change in the rain ratio that was more likely a consequence than a cause of climate change.

10. Conclusions

The geographic extent and intensity of deposition of laminated diatom mat deposits (LDM) are used to track the position of the Antarctic Polar Front during the mid- to late Pleistocene. These deposits corroborate previous evidence of frontal migration based on changes in sediment composition, microfossil distribution and palaeotemperature estimates. The LDM track glacial-interglacial meridional movement of the APF commonly of at least 3 and, on occasion, more than 6 degrees in the mid- and late Pleistocene.

Starting at about 900 ka (MIS 22) from a locus during interglacials and transitions spanning 47° to 50° South, the APF at a longitude of 7° East, underwent a stepwise minimum 7° migration to the north over a period of about 150 kyr and held a sustained northerly position until returning abruptly south following MIS 12 during Termination V at 424 ka to a (deglacial and interglacial) locus spanning 50° to 53° South. This period or "Mid-Pleistocene Interim State" spanning the interval from a 900 ka event that saw major cooling of the oceans and a δ^{13}C minimum, to the 424 ka

Mid-Brunhes Event is also characterised by the following: more intense and longer glaciations than previously; lower oxygen isotope peaks (higher values) during interglacials showing evidence for less complete deglaciations than before or after; reduced mean flow of the Deep Western Boundary Current in the southwest Pacific evidencing sluggish renewal of deep waters; sustained decreased carbonate in the sub-tropical South Atlantic evidencing increased SCW / reduced NADW influence; a reconfiguration of the African monsoon with increased aridity and, for the interval for which ice core records are available (800 ka), lower interglacial temperatures and lower interglacial atmospheric CO_2 levels (by some 30 per mil) than those following MIS 12.

Taken together this evidence is consistent with an extension of Toggweiler's "Midlatitude Westerlies, Atmospheric CO_2" hypothesis (Toggweiler et al., 2006) from glacial-interglacial cycles to this longer interval of the mid-Pleistocene transition, at least in its proposition of a link between the latitude of the westerlies and the depth horizon of ventilation in the ocean basins north of that latitude. Essentially, in the context of this hypothesis, from MIS 22 to MIS 12 (the approximate period 900-424 ka), the westerlies were situated too far north, even during interglacials, to fully ventilate the deep ocean (Fig. 7).

The cooling that initiated this "mid Pleistocene interim state of ocean circulation" was likely driven by a drop in insolation amplitude following 950 ka related to eccentricity modulation of precession. The sequence and timing of cooling episodes point to an interplay between 400 kyr and 100 kyr eccentricity modulation of precession. Intriguingly, the initial "900 ka" event of the MPT was initiated by insolation minima related to a 100 kyr eccentricity modulation of precession that preceded a broader minima in insolation amplitude centred around the 800 ka, 400 kyr eccentricity modulation (Fig. 6). The latter was likely responsible for the additional cooling and sustained duration of the Mid Pleistocene Interim State. Through this interval it is therefore likely that the carbon cycle was responding to reconfigurations of the earth system driven by changes of insolation forcing related to eccentricity modulation of precession.

Acknowledgements

Figure Captions

Figure 1

Location of main Leg 177 sites discussed in text showing bathymetry and present position of major fronts.

Figure 2

Water column and core topographic SEM images of *Thalassiothrix antarctica* mats. a) A tangled mass of *T. antarctica* (some frustules in sheaves) sampled from 100 m depth in 1982 at 66° 38', S 72° 57' E above the Antarctic shelf edge. Image courtesy of Gustaaf Hallegraef (Hallegraef, 1986). Scale bar – 1 mm. b) A series of *T. antarctica* mats from core interval 1093A-30H-1, 62-66 cm. Scale bar - 100 microns. The centric diatom also present is *Thalassiosira lentiginosa*.

Figure 3

Back scattered electron images showing fabrics of Leg 177 sediments. (Scale bar in d applies to all images.) a) Laminated diatom mat (LDM) sediment showing pervasive discrete laminae corresponding to depositional episodes and lamina-parallel partings. Blizzard appearance is due to the abundance of cross sections of the *Thalassiothrix* frustule (compare Fig. 2) and highlights the very porous nature of the LDM. (MIS 27 in Site 1093; polished thin section (PTS) is within core interval 1093A-23H-4, 0-22cm). b) Intermittent laminated diatom mat deposits with LDM intervals indicated by black bars. These are darker in BSEI (more porous) than the intervening sediment with more mixed diatom assemblages and pellets showing influence of bioturbation. (MIS 27 in Site 1091; PTS is within core interval 1091A-13H-5, 130-140 cm). c) Near homogeneous siliceous ooze in which fragments of mats are visible (labelled). (Holocene sediments, Site 1093; PTS is within core interval 1093C-2H-3, 80-112cm) d) Interval of LDM within homogeneous and burrowed siliceous ooze. LDM, indicated by a black bar, is characterised by darker BSEI (higher porosity) and laminae. The LDM interval is on the boundary of two successive polished thin sections with oblique cuts to ensure continuity in observation. (Termination V, MIS 12-11, Site 1093; PTS within core interval 1093A-13H-4, 0-18cm).

Figure 4

Occurrence and correlation of laminated diatom mat deposits in sites 1091, 1093 and 1094 over the past 1100 kyr (see key in Figure for degree of preservation of LDM). The curves in all sites are of red reflectance. Isotope stages are labelled and the LRO4 stack (Lisiecki and Raymo, 2005) is included for reference.

Figure 5

Summary of major Polar Front migrations over the past 1100 kyr in relation to other records through the Mid Pleistocene Transition and Mid Brunhes Event. (a) Schematic migration of the Antarctic Polar Front at around 5° East based on the LDM occurrence of Fig. 5. Note the latitude of the 3 ODP Sites (1091, 1093, 1094) used to track the front are indicated and the shaded zone marks the main deglacial and interglacial locus (see Figure 3 and text); (b) Sortable Silt grain size from the Chatham Drift, a proxy for Deep Western Boundary Current mean flow speed. The lines indicate the mean values for the periods 0-450 ka; 450 – 870 ka and 870 – 1190 ka from Hall et al. (2001); (c) δ^{18}O of *Globorotalia inflata* from ODP Site 1082 showing changes in Benguela Coastal Current sea surface temperatures [record of Jahn et al. (2003) as updated by J. Etourneau, written comm. (2008)]. The lines indicate mean values for the periods 0-420 ka; 420-770 ka and 770-1110 kyr; (d) Stacked, smoothed benthic foraminiferal δ^{13}C from Hoogakker et al. (2006); (e) Composite atmospheric CO_2 from Antarctic ice cores from following sources, 0-22 ka: EPICA Dome C (Monnin et al., 2001), 22-393 ka: Vostok (Petit et al., 1999; Pepin et al., 2000; Raynaud et al., 2005); 393-664 ka: EPICA Dome C, (Siegenthaler et al., 2005); 664-800 ka: Dome C (Luthi et al., 2008); (f) Stacked benthic oxygen isotope curve from (Lisiecki and Raymo, 2005); (g) Summer (June-July) insolation at 65° North of Laskar et al. (2004) taken from the Analyseries program (Paillard et al., 1996). All records are presented on their published age models.

Figure 6

Detail of the initiation of the MPT showing the sequence of events around the "900 ka event" and the relation of these to insolation changes. Top graph (a) shows evidence for a step increase in dust input to Mediterranean from Larrasoana et al. (2003) due to increased aridification because of reduced northern penetration of the monsoon. This switch in monsoon threshold is driven by a cooling due to reduced insolation during precession minima (graphs (c) and (d)). (b) Sequence of events at the start of the MPT leading to the "900 ka event" and including major migrations of the Antarctic Polar Front evidenced by changes in the locus of LDM deposition. Insolation profiles for 65° N summer (c) and for 65° S summer (d). Both insolation profiles are from Laskar et al. (2004) taken from the Analyseries program (Paillard et al., 1996). The markings e100 and e400 denote respectively100 kyr and 400 kyr period eccentricity modulation of precession resulting in intervals of minimum insolation amplitude.

Figure 7

Schematic of the inferred surface circulation (above) and overturning circulation (below) of the Southern Ocean in an interglacial stage (left) after or before and (right) during the MPT. Red / blue shading is indicative of warm / cool temperatures, and the relative thickness of arrows denotes the strength of the circulation. The thick grey arrows mark the latitude of the Southern Ocean westerlies. SB – southern boundary of the ACC.

SUPPLEMENTARY FIGURE CAPTION

Figure S-1

Age model calculations. a) depth-depth plots between Site 1094 (master) and Sites 1091 & 1093, of all available biostratigraphic, paleomagnetic and oxygen isotope data. Using multiple polynomials the high dating density of Site 1094 was transferred to the other sites (see text for discussion of method). b) Site 1091 age-depth plots and best fit polynomials, c) Site 1093 age-depth plots and best fit polynomials, d) Site 1094 age-depth plots and best fit polynomials.

References

Anderson, R.F., Ali, S., Bradtmiller, L.I., Nielsen, S.H.H., Fleisher, M.Q., Anderson, B.E. and Burckle, L.H., 2009. Wind-Driven Upwelling in the Southern Ocean and the Deglacial Rise in Atmospheric CO2. Science, 323(5920): 1443-1448.

Anderson, R.F., Chase, Z., Fleisher, M.Q. and Sachs, J., 2002. The Southern Ocean's biological pump during the Last Glacial Maximum. Deep-Sea Research Part II-Topical Studies in Oceanography, 49(9-10): 1909-1938.

Bard, E. and Rickaby, R.E.M., 2009. Migration of the subtropical front as a modulator of glacial climate. Nature, 460(7253): 380-U93.

Becquey, S. and Gersonde, R., 2002. Past hydrographic and climatic changes in the Subantarctic Zone of the South Atlantic - The Pleistocene record from ODP Site 1090. Palaeogeography Palaeoclimatology Palaeoecology, 182(3-4): 221-239.

Berger, A., Melice, J.L. and Loutre, M.F., 2005. On the origin of the 100-kyr cycles in the astronomical forcing. Paleoceanography, 20(4): doi:10.1029/2005PA001173.

Berger, W.H. and Jansen, E., 1994. Mid-Pleistocene Climate Shift - the Nansen Connection. In: M. Johannesen, R.D. Muench and J.E. Overland (Editors), The Polar Oceans and their role in shaping the global environment. Geophysical Monograph Series. American Geophysical Union, pp. 295-311.

Bianchi, C. and Gersonde, R., 2002. The Southern Ocean surface between Marine Isotope Stages 6 and 5d: Shape and timing of climate changes. Palaeogeography Palaeoclimatology Palaeoecology, 187(1-2): 151-177.

Böning, C.W., Dispert, A. , Visbeck, M., Rintoul, S.R. and Schwarzkopf, F.U., 2008. The response of the Antarctic Circumpolar current to recent climate change. Nature Geoscience, 1, 864-869.

Burckle, L.H., 1984. Diatom Distribution and Paleoceanographic Reconstruction in the Southern-Ocean - Present and Last Glacial Maximum. Marine Micropaleontology, 9(3): 241-261.

Burckle, L.H. and Cirilli, J., 1987. Origin of Diatom Ooze Belt in the Southern-Ocean - Implications for Late Quaternary Paleoceanography. Micropaleontology, 33(1): 82-86.

Channell, J.E.T. and Stoner, J.S., 2002. Plio-Pleistocene magnetic polarity stratigraphies and diagenetic magnetite dissolution at ODP Leg 177 Sites (1089, 1091, 1093 and 1094). Marine Micropaleontology, 45(3-4): 269-290.

Charles, C.D., Froelich, P.N., Zibello, M.A., Mortlock, R.A. and Morley, J.J., 1991. Biogenic opal in Southern Ocean sediments over the last 450,000 years: implications for surface water chemistry and circulation. Paleoceanography, 6: 697-728.

Ciesielski, P.F. and Weaver, F.M., 1983. Neogene and Quaternary paleoenvironmental history of Deep Sea Drilling Project Leg 71 sediments, southwest Atlantic Ocean. In: L.J. Ludwig and V.A. Kasheninnikov (Editors), Init. Repts. DSDP. U.S. Govt. Printing Office, Washington, pp. 461-477.

Clark, P.U., Archer, D., Pollard, D., Blum, J.D., Rial, J.A., Brovkin, V., Mix, A.C., Pisias, N.G. and Roy, M., 2006. The middle Pleistocene transition: characteristics. mechanisms, and implications for long-term changes in atmospheric PCO2. Quaternary Science Reviews, 25(23-24): 3150-3184.

Cortese, G., Gersonde, R., Hillenbrand, C.D. and Kuhn, G., 2004. Opal sedmentation shifts in the World Ocean over the last 15 Myr. Earth and Planetary Science Letters, 224: 509-527.

Cortese, G. and Gersonde, R., 2008. Plio/Pleistocene changes in the main biogenic silica carrier in the Southern Ocean, Atlantic Sector. Marine Geology, 252(3-4): 100-110.

Crucifix, M., Loutre, M.F. and Berger, A., 2006. The climate response to the astronomical forcing. Space Science Reviews, 125(1-4): 213-226.

de Boer, A.M., Sigman, D.M., Toggweiler, J.R. and Russell, J.L., 2007. Effect of global ocean temperature change on deep ocean ventilation. Paleoceanography, 22(2): doi:10.1029/2005PA001242.

Deacon, G.E.R., 1982. Physical and Biological Zonation in the Southern-Ocean. Deep-Sea Research Part a-Oceanographic Research Papers, 29(1): 1-15.

Dean, J.M., Kemp, A.E.S., Bull, D., Pike, J., Pettersen, G. and Zolitchka, B., 1999. Taking varves to bits: Scanning electron microscopy in the study of laminated sediments and varves. Journal of Paleolimnology, 22(2): 121-136.

Dean, J.M., Kemp, A.E.S. and Pearce, R.B., 2001. Palaeo-flux records from electron microscope studies of Holocene laminated sediments, Saanich Inlet, British Columbia. Marine Geology, 174(1-4): 139-158.

DeMaster, D.J., 2002. The accumulation and cycling of biogenic silica in the
Southern Ocean: revisiting the marine silica budget. Deep-Sea Research Part
Ii-Topical Studies in Oceanography, 49(16): 3155-3167.

Diekmann, B. and Kuhn, G., 2002. Sedimentary record of the mid-Pleistocene climate
transition in the southeastern South Atlantic (ODP Site 1090).
Palaeogeography Palaeoclimatology Palaeoecology, 182(3-4): 241-258.

Dong, S., Sprintall, J. and Gille, S., 2006. Location of the Polar Front from AMSR-E
satellite surface temperature measurements. Journal of Physical
Oceanography, 36(11): 2075-2089.

Edwards, L., 1984. Insights on why graphic correlation (Shaw's method) works.
Journal of Geology, 92: 583-597.

EPICA, community and members, 2004. Eight glacial cycles from an Antarctic ice
core. Nature, 429: 623-628.

Fenner, J., Schrader, H.-J. and Wienigk, H., 1976. Diatom phytoplankton studies in
the Southern Pacific Ocean, composition and correlation to the Antarctic
convergence and its palaeoecological significance. In: C.D. Hollister and C.
Craddock (Editors), Initial Reports of the Deep Sea Drilling Project. U.S.
Government Printing Office, Washington, pp. 757-784.

Fenner, J.M., 1991. Late Pliocene-Quaternary quantitative diatom stratigraphy in the
Atlantic sector of the Southern Ocean. Proceedings of the Ocean Drilling
Program, Scientific Results., 114: 97-122.

Flores, J.A. and Marino, M., 2002. Pleistocene calcareous nannofossil stratigraphy for
ODP Leg 177 (Atlantic sector of the Southern Ocean). Marine
Micropaleontology, 45(3-4): 191-224.

Flores, J.A. and Sierro, F.J., 2007. Pronounced mid-Pleistocene southward shift of the
Polar Front in the Atlantic sector of the Southern Ocean. Deep-Sea Research
Part Ii-Topical Studies in Oceanography, 54(21-22): 2432-2442.

Fyfe, J.C. and Saenko, O.A., 2005. Human-induced change in the Antarctic
Circumpolar Current. Journal of Climate, 18(15): 3068-3073.

Fyfe, J.C., Saenko, O.A., Zickfield, K., Eby, M. and Weaver, A., 2007. The role of
poleward intensifying winds on Southern Ocean warming. Journal of Climate,
20: 5391-5400.

Gersonde, R., Abelmann, A., Brathauer, U., Becquey, S., Bianchi, C., Cortese, G.,
Grobe, H., Kuhn, G., Niebler, H.S., Segl, M., Sieger, R., Zielinski, U. and

Futterer, D.K., 2003. Last glacial sea surface temperatures and sea-ice extent in the Southern Ocean (Atlantic-Indian sector): A multiproxy approach. Paleoceanography, 18(3): doi:10.1029/2002PA000809.

Gersonde, R., Crosta, X., Abelmann, A. and Armand, L., 2005. Sea-surface temperature and sea ice distribution of the Southern Ocean at the EPILOG Last Glacial Maximum - A circum-Antarctic view based on siliceous microfossil records. Quaternary Science Reviews, 24(7-9): 869-896.

Gersonde, R. and Hodell, D.A., 2002. Southern Ocean Paleoceanography - Insights from Ocean Drilling Program Leg 177. Palaeogeography Palaeoclimatology Palaeoecology, 182(3-4): 145-149.

Gingele, F.X. and Schmieder, F., 2001. Anomalous South Atlantic lithologies confirm global scale of unusual mid-Pleistocene climate excursion. Earth and Planetary Science Letters, 186(1): 93-101.

Govin, A., Michel, E., Labeyrie, L., Waelbroeck, C., Dewilde, F. and Jansen, E., 2009. Evidence for northward expansion of Antarctic Bottom Water mass in the Southern Ocean during the last glacial inception. Paleoceanography, 24: doi:10.1029/2008PA001603.

Grigorov, I., 2004. Southern Ocean Palaeoceanography from Thalassiothrix antarctica deposits. PhD Thesis, University of Southampton, Southampton, 139 pp.

Grigorov, I., Pearce, R.B. and Kemp, A.E.S., 2002. Southern Ocean laminated diatom ooze: mat deposits and potential for palaeo-flux studies, ODP leg 177, Site 1093. Deep-Sea Research Part II-Topical Studies in Oceanography, 49(16): 3391-3407.

Hall, A. and Visbeck, M., 2002. Synchronous variability in the southern hemisphere atmosphere, sea ice, and ocean resulting from the annular mode. Journal of Climate, 15(21): 3043-3057.

Hall, I.R., McCave, I.N., Shackleton, N.J., Weedon, G.P. and Harris, S.E., 2001. Intensified deep Pacfic inflow and ventilation in Pleistocene glacial times. Nature, 412(6849): 809-812.

Hallberg, R. and Gnanadesikan, A., 2006. The role of eddies in determining the structure and response of the wind-driven southern hemisphere overturning: Results from the Modeling Eddies in the Southern Ocean (MESO) project. Journal of Physical Oceanography, 36(12): 2232-2252.

Hallegraef, G.M., 1986. Taxonomy and morphology of the marine planktonic diatoms *Thalassionema* and *Thalassiothrix*. Diatom Research, 1, 57-80.

Hayward, B.W., Kawagata, S., Grenfell, H.R., Sabaa, A.T. and O'Neill, T., 2007. Last global extinction in the deep sea during the mid-Pleistocene climate transition. Paleoceanography, 22(3): doi:10.1029/2007PA001424.

Hemming, S.R. et al., 2007. Strontium isotope tracing of terrigenous sediment dispersal in the Antarctic Circumpolar Current: Implications for constraining frontal positions. Geochemistry, Geophysics, Geosystems, 8(6): doi:10.1029/2006GC001441.

Hodell, D.A. et al., 2003a. Data Report: Oxygen Isotope Stratigraphy of ODP Leg 177 Sites 1088,1089, 1090, 1093, and 1094. In: R. Gersonde, D.A. Hodell and P. Blum (Editors), Proc. ODP, Sci. Results, . Available from: Ocean Drilling Program, Texas A&M University, College Station, TX.

Hodell, D.A., Venz, K.A., Charles, C.D. and Ninnemann, U.S., 2003b. Pleistocene vertical carbon isotope and carbonate gradients in the South Atlantic sector of the Southern Ocean. Geochemistry Geophysics Geosystems, 4: doi:10.1029/2002GC000367.

Hönisch, B., Hemming, N.G., Archer, D., Siddall, M. and McManus, J.F., 2009. Atmospheric Carbon Dioxide Concentration Across the Mid-Pleistocene Transition. Science, 324(5934): 1551-1554.

Hoogakker, B.A.A., Rohling, E.J., Palmer, M.R., Tyrrell, T. and Rothwell, R.G., 2006. Underlying causes for long-term global ocean delta C-13 fluctuations over the last 1.20 Myr. Earth and Planetary Science Letters, 248(1-2): 15-29.

Howard, W.R. and Prell, W.L., 1992. Late Quaternary surface circulation of the Southern Indian Ocean and its relation to orbital variations. Paleoceanography, 7: 79-118.

Hughes, C.W. and Ash, E.R., 2001. Eddy forcing of the mean flow in the Southern Ocean. Journal of Geophysical Research-Oceans, 106(C2): 2713-2722.

Hutchins, D.A, Sedwick, P.N., DiTullo, G.R., Boyd, P.W., Queguiner, B. Griffiths, F.B. and Crossley, C., 2001. Control of phytoplankton growth by iron and silicic acid availability in the subantarctic Southern Ocean: Experimental results from the SAZ Project. Journal of Geophysical Research-Oceans, 106(C12): 31559-31572.

Jahn, B., Donner, B., Muller, P.J., Rohl, U. Schneider, R.R. and Wefer, G., 2003. Pleistocene variations in dust input and marine productivity in the northern Benguela Current: Evidence of evolution of global glacial-interglacial cycles. Palaeogeography Palaeoclimatology Palaeoecology, 193(3-4): 515-533.

Jansen, J.H.F., Kuijpers, A. and Troelstra, S.R., 1986. A Mid-Brunhes Climatic Event - Long-Term Changes in Global Atmosphere and Ocean Circulation. Science, 232(4750): 619-622.

Jouzel, J. et al., 2007. Orbital and millennial Antarctic climate variability over the past 800,000 years. Science, 317(5839): 793-796.

Kanfoush, S.L., Hodell, D.A., Charles, C.D., Janecek, T.R. and Rack, F.R., 2002. Comparison of ice-rafted debris and physical properties in ODP Site 1094 (South Atlantic) with the Vostok ice core over the last four climatic cycles. Palaeogeography Palaeoclimatology Palaeoecology, 182(3-4): 329-349.

Kemp, A.E.S. and Baldauf, J.G., 1993. Vast Neogene laminated diatom mat deposits from the eastern equatorial Pacific Ocean. Nature, 362: 141-144.

Kemp, A.E.S., Pearce, R.B., Grigorov, I., Rance, J., Lange, C.B., Quilty, P. and Salter, I., 2006. Production of giant marine diatoms and their export at oceanic frontal zones: Implications for Si and C flux in stratified oceans. Global Biogeochemical Cycles, 20: doi:10.1029/2006GB002698.

Kemp, A.E.S., Pike, J., Pearce, R.B. and Lange, C.B., 2000. The "Fall dump" - a new perspective on the role of a "shade flora" in the annual cycle of diatom production and export flux. Deep-Sea Research Part II-Topical Studies in Oceanography, 47: 2129-2154.

King, S.C., Kemp, A.E.S. and Murray, J.W., 1995. Changes in benthic foraminifer assemblages through Neogene laminated diatom ooze deposits in the eastern equatorial Pacific Ocean (ODP Site 844). In: N.G. Pisias, L.A. Mayer, T.R. Janecek and e. al. (Editors), Proceedings of ODP Scientific Results, 138. College Station, TX (Ocean Drilling Program), pp. 655-673.

Klaas, C., Kuhn, S., Menden-Deuer, T., Reynarson, T. and Smetacek, V., 1997. Phytoplankton and Heterotrphic protist counts. Bereich Polarforschung, 221: 68-71.

Kleiven, H.F. and Jansen, E., 2003. Data report: Early-mid-Pleistocene oxygen isotope stratigraphy from the Atlantic sector of the southern ocean; ODP Leg

177 Sites 1094 AND 1091. Proceedings of the Ocean Drilling Program, Scientific Results, 177: [Online].

Kleiven, H.F., Jansen, E., Curry, W.B., Hodell, D.A. and Venz, K., 2003. Atlantic Ocean thermohaline circulation changes on orbital to suborbital timescales during the mid-Pleistocene. Paleoceanography, 18(1): doi:10.1029/2001PA000629.

Kohler, P. and Fischer, H., 2006. Simulating low frequency changes in atmospheric CO2 during the last 740 000 years. Climate of the Past, 2(2): 57-78.

Kopczynska, E.E., Dehairs, F., Elskens, M. and Wright, S., 2001. Phytoplankton and microzooplankton variability between the Subtropical and Polar Fronts south of Australia: Thriving under regenerative and new production in late summer. Journal of Geophysical Research-Oceans, 106(C12): 31597-31609.

Kuhn, G. and Diekmann, B., 2002. Late Quaternary variability of ocean circulation in the southeastern South Atlantic inferred from the terrigenous sediment record of a drift deposit in the southern Cape Basin (ODP Site 1089). Palaeogeography Palaeoclimatology Palaeoecology, 182: 287-303.

Kunz-Pirrung, M., Gersonde, R. and Hodell, D.A., 2002. Mid-Brunhes century-scale diatom sea surface temperature and sea ice records from the Atlantic sector of the Southern Ocean (ODP Leg 177, sites 1093, 1094 and core PS2089-2). Palaeogeography Palaeoclimatology Palaeoecology, 182(3-4): 305-328.

Larrasoana, J.C., Roberts, A.P., Rohling, E.J., Winklhofer, M. and Wehausen, R., 2003. Three million years of monsoon variability over the northern Sahara. Climate Dynamics, 21(7-8): 689-698.

Laskar, J., Robutel, P., Joutel, F., Gastineau, M., Correia, A.C.M. and Levrard, B., 2004. A long-term numerical solution for the insolation quantities of the Earth. Astronomy & Astrophysics, 428(1): 261-285.

Li, Q.Y., Wang, P.X., Zhao, Q.H., Tian, J., Cheng, X.R., Jian, Z.M., Zhong, G.F. and Chen, M.H., 2008. Paleoceanography of the mid-Pleistocene South China Sea. Quaternary Science Reviews, 27(11-12): 1217-1233.

Lisiecki, L.E. and Raymo, M.E., 2005. A Pliocene-Pleistocene stack of 57 globally distributed benthic delta O-18 records. Paleoceanography, 20(1): doi:10.1029/2004PA001071.

Lourens, L.J., 2004. Revised tuning of Ocean Drilling Program Site 964 and KC01B (Mediterranean) and implications for the delta O-18, tephra, calcareous

nannofossil, and geomagnetic reversal chronologies of the past 1.1 Myr. Paleoceanography, 19(3): doi:10.1029/2003PA000997.

Luthi, D. et al., 2008. High-resolution carbon dioxide concentration record 650,000 - 800,000 years before present. Nature, 453: 379-382.

Marchitto, T.M., Lehman, S.J., Ortiz, J.D., Fluckiger, J. and van Geen, A., 2007. Marine radiocarbon evidence for the mechanism of deglacial atmospheric CO2 rise. Science, 316(5830): 1456-1459.

Martinez-Garcia, A., Rosell-Mele, A., Geibert, W., Gersonde, R., Masque, P., Gaspari and Barbante, C., 2009. Links between iron supply, marine productivity, sea surface temperature, and CO2 over the last 1.1 Ma. Paleoceanography, 24: doi:10.1029/2008PA001657.

McClymont, E.L. and Rosell-Mele, A., 2005. Links between the onset of modern Walker circulation and the mid-Pleistocene climate transition. Geology, 33(5): 389-392.

Medina-Elizalde, M. and Lea, D.W., 2005. The mid-Pleistocene transition in the tropical Pacific. Science, 310(5750): 1009-1012.

Monnin, E. et al., 2001. Atmospheric CO2 concentrations over the last glacial termination. Science, 291(5501): 112-114.

Moore, J.K., Abbott, M.R., Richman, J.G. and Nelson, D.M., 2000. The Southern Ocean at the last glacial maximum: A strong sink for atmospheric carbon dioxide. Global Biogeochemical Cycles, 14(1): 455-475.

Morley, J.J., 1989. Variations in high latitude oceanographic fronts in the Southern Indian Ocean: an estimation based on faunal changes. Paleoceanography, 4: 547-554.

Mudelsee, M. and Schulz, M., 1997. The Mid-Pleistocene climate transition: onset of 100 ka cycle lags ice volume build-up by 280 ka. Earth and Planetary Science Letters, 151(1-2): 117-123.

Mudelsee, M. and Stattegger, K., 1997. Exploring the structure of the mid-Pleistocene revolution with advanced methods of time series analysis. Geologische Rundschau, 86(2): 499-511.

Naveira Garabato, A.C.N., Strass, V.H. and Kattner, G., 2002. Fluxes of nutrients in a three-dimensional meander structure of the Antarctic Polar Front. Deep-Sea Research Part II-Topical Studies in Oceanography, 49(18): 3771-3792.

Nelson, D.M., Brzezinski, M.A., Sigmon, D.E. and Franck, V.M., 2001. A seasonal progression of Si limitation in the Pacific sector of the Southern Ocean. Deep-Sea Research Part Ii-Topical Studies in Oceanography, 48(19-20): 3973-3995.

O'Neill, T.A., Hayward, B.W., Kawagata, S., Sabaa, A.T. and Grenfell, H.R., 2007. Pleistocene extinctions of deep-sea benthic foraminifera: The south Atlantic record. Palaeontology, 50: 1073-1102.

Oke, P.R. and England, M.H., 2004. Oceanic response to changes in the latitude of the Southern Hemisphere subpolar westerly winds. Journal of Climate, 17(5): 1040-1054.

Orsi, A.H., Whitworth III, T. and Nowlin, W.D.J., 1995. On the meridional extent and fronts of the Antarctic Circumpolar Current. Deep-Sea Research I, 42: 641-673.

Paillard, D., Labeyrie, L. and Yiou, P., 1996. Macintosh program performs time-series analysis. Eos, Trans. American Geophysical Union, 77: 379.

Pälike, H., Norris, R.D., Herrle, J.O., Wolsion, P.A., Coxall, H.K., Lear C.H., Shackleton, N.J., Tripati, A.K. and Wade, B.S., 2006. The heartbeat of the oligocene climate system. Science, 314(5807): 1894-1898.

Parslow, J.S., Boyd, P.W., Rintoul, S.R. and Griffiths, F.B., 2001. A persistent subsurface chlorophyll maximum in the Interpolar Frontal Zone south of Australia: Seasonal progression and implications for phytoplankton-light-nutrient interactions. Journal of Geophysical Research-Oceans, 106(C12): 31543-31557.

Peeters, F.J.C., Acheson, R., Brunner, G.J.A., de Ruijter, W.P. schneider, R.R., Ganssen, G.M., Ufkes, E. and Kroon, D., 2004. Vigorous exchange between the Indian and Atlantic oceans at the end of the past five glacial periods. Nature, 430(7000): 661-665.

Pepin, L., Barnola, J.M., Petit, J.R. and Raynaud, D., 2000. Time evolutions of the greenhouse effect gases concentration and the climate from the Vostok core. Houille Blanche-Revue Internationale De L Eau(3-4): 64-67.

Petit, J.R. et al., 1999. Climate and atmospheric history of the past 420,000 years from the Vostok ice core, Antarctica. Nature, 399: 429-436.

Pike, J. and Kemp, A.E.S., 1999. Diatom mats from Gulf of California: Implications for silica burial and paleoenvironmental interpretation of laminated sediments. Geology, 27: 311-314.

Pollard, R.T., Lucas, M.I. and Read, J.F., 2002. Physical controls on biogeochemical zonation in the Southern Ocean. Deep-Sea Research Part II-Topical Studies in Oceanography, 49(16): 3289-3305.

Raymo, M.E., Oppo, D.W. and Curry, W., 1997. The mid-Pleistocene climate transition: A deep sea carbon isotopic perspective. Paleoceanography, 12(4): 546-559.

Raynaud, D., Barnola, J.M., Souchez, R., Lorrain, R., Petit, J.R. Duval, P. and Lipenkov, V.Y., 2005. Palaeoclimatology - The record for marine isotopic stage 11. Nature, 436(7047): 39-40.

Rintoul, S.R., Hughes, C.W. and Olbers, D., 2001. The Antarctic Circumpolar Current system. In: G. Siedler, J. Church and J. Gould (Editors), Ocean circulation and climate: observing and modelling the global ocean. Academic Press, New York.

Rintoul, S.R. and Sokolov, S., 2001. Baroclinic transport variability of the Antarctic Circumpolar Current south of Australia (WOCE repeat section SR3). Journal of Geophysical Research-Oceans, 106(C2): 2815-2832.

Rohling, E.J., Fenton, M. Jorrisen, F.J., Bertrand, P. Ganssen and Caulet, J.P., 1998. Magnitudes of sea-level lowstands of the past 500,000 years. Nature, 394: 162-165.

Romero, O. and Schmieder, F., 2006. Occurrence of thick Ethmodiscus oozes associated with a terminal Mid-Pleistocene Transition event in the oligotrophic subtropical South Atlantic. Palaeogeography Palaeoclimatology Palaeoecology, 235(4): 321-329.

Russell, J.L., Dixon, K.W., Gnanadesikan, A., Toggweiler, J.R. and Stouffer, R.J., 2006. The once and future battles between thor and the midgard serpent: The Southern Hemisphere Westerlies and the Antarctic Circumpolar Current. Geochimica Et Cosmochimica Acta, 70(18): A547-A547.

Saenko, O.A., Fyfe, J.C. and England, M.H., 2005. On the response of the oceanic wind-driven circulation to atmospheric CO_2 increase. Climate Dynamics, 25(4): 415-426.

Sallée, J.B., Speer, K. and Morrow, R., 2008. Response of the Antarctic Circumpolar Current to atmospheric variability. Journal of Climate, 21: 3020-3039.

Sarmiento, J.L., Gruber, N., Brzezinski, M.A. and Dunne, J.P., 2004. High-latitude controls of thermocline nutrients and low latitude biological productivity. Nature, 427(6969): 56-60.

Schefuss, E., Damste, J.S.S. and Jansen, J.H.F., 2004. Forcing of tropical Atlantic sea surface temperatures during the mid-Pleistocene transition. Paleoceanography, 19(4): doi:10.1029/2003PA000892.

Schefuss, E., Schouten, S., Jansen, J.H.F. and Damste, J.S.S., 2003. African vegetation controlled by tropical sea surface temperatures in the mid-Pleistocene period. Nature, 422(6930): 418-421.

Scherer, R.P., Bohaty, S.M., Dunbar, G.B., Esper, O., Flores, J.-A., Gersonde, R., Harwood, D.M., Roberts, A.P. and Taviani, M. 2008. Antarctic records of precessin-paced insolation-driven warming during early Pleistocene Marine Isotope Stage 31. Geophysical Research Letters, 35, doi:10.1029/2007GL032254.

Schluter, M., van der Loeff, M.M.R., Holby, O. and Kuhn, G., 1998. Silica cycle in surface sediments of the South Atlantic. Deep-Sea Research Part I-Oceanographic Research Papers, 45(7): 1085-1109.

Schmieder, F., von Dobeneck, T. and Bleil, U., 2000. The Mid-Pleistocene climate transition as documented in the deep South Atlantic Ocean: initiation, interim state and terminal event. Earth and Planetary Science Letters, 179(3-4): 539-549.

Schneider-Mor, A., Yam, R. Bianchi, C., Kunz-Pirrung, M., Gersonde, R. and Shemesh, A. 2005. Diatom stable isotopes, sea ice presence and sea surface temperature records of the past 640 ka in the Atlantic sector of the Southern Ocean. Geophysical Research Letters, 32(L10704): doi:10.1029/2005GL022543.

Schrader, H.-J., 1974. Proposal for a standardized method of cleaning diatom-bearing deep-sea and land-exposed marine sediments. Nova Hedwigia, 45: 403-409.

Shackleton, N.J., 2000. The 100,000-year ice-age cycle identified and found to lag temperature, carbon dioxide, and orbital eccentricity. Science, 289(5486): 1897-1902.

Shaw, A.B., 1964. Time in Stratigraphy. McGraw Hill, New York, 365 pp.

Shipboard-Scientific-Party, 1999. Leg 177 summary: Southern Ocean paleoceanography. Proceedings of the Ocean Drilling Program, Initial Reports, 177: 1-67.

Siegenthaler, U. et al., 2005. Stable carbon cycle-climate relationship during the late Pleistocene. Science, 310(5752): 1313-1317.

Sijp, W.P. and England, M.H., 2008. The effect of a northward shift in the Southern Hemisphere westerlies on the global ocean. Progress in Oceanography, in press.

Sinha, B. and Richards, K.J., 1999. Jet structure and scaling in southern ocean models. Journal of Physical Oceanography, 29(6): 1143-1155.

Strass, V.H. et al., 2002. Mesoscale frontal dynamics: shaping the environment of primary production in the Antarctic Circumpolar Current. Deep-Sea Research Part II-Topical Studies in Oceanography, 49(18): 3735-3769.

Toggweiler, J.R., 1999. Variation of atmospheric CO2 by ventilation of the ocean's deepest water. Paleoceanography, 14(5): 571-588.

Toggweiler, J.R., 2009. Shifting Westerlies. Science, 323(5920): 1434-1435.

Toggweiler, J.R., Russell, J.L. and Carson, S.R., 2006. Midlatitude westerlies, atmospheric CO2, and climate change during the ice ages. Paleoceanography, 21(2): doi:10.1029/2005PA001154.

Treguer, P., Nelson, D.M., van Bennekom, A.J., DeMaster, D.J., Leynaert, A. and Queguiner, B 1995. The silica balance in the world ocean : A reestimate. Science, 268: 377-379.

Treguier, A.M. and Panetta, R.L., 1994. Multiple Zonal Jets in a Quasi-Geostrophic Model of the Antarctic Circumpolar Current. Journal of Physical Oceanography, 24(11): 2263-2277.

Tremblay, J.E., Lucas, M.I., Kattner, G., Pollard, R., Strass, V.H., Bathmann, U. and Bracher, A. 2002. Significance of the Polar Frontal Zone for large-sized diatoms and new production during summer in the Atlantic sector of the Southern Ocean. Deep-Sea Research Part II-Topical Studies in Oceanography, 49(18): 3793-3811.

Tziperman, E. and Gildor, H., 2003. On the mid-Pleistocene transition to 100-kyr glacial cycles and the asymmetry between glaciation and deglaciation times. Paleoceanography, 18(1): doi:10.1029/2001PA000627.

Venuti, A., Florindo, F., Michel, E. and Hall, I.R., 2007. Magnetic proxy for the deep (Pacific) western boundary current variability across the mid-Pleistocene climate transition. Earth and Planetary Science Letters, 259(1-2): 107-118.

Venz, K.A. and Hodell, D.A., 2002. New evidence for changes in Plio-Pleistocene deep water circulation from Southern Ocean ODP Leg 177 Site 1090. Palaeogeography Palaeoclimatology Palaeoecology, 182(3-4): 197-220.

Wang, P., Tian, J., Change, X., Liu, C. and Xu, J., 2004. Major Pleistocene stages in a carbon perspective: The South China Sea record and its global comparison. Paleoceanography, 19(4): doi:10.1029/2003PA000991.

Wang, P.X., Tian, J., Cheng, X.R., Liu, C.L. and Xu, J., 2003. Carbon reservoir changes preceded major ice-sheet expansion at the mid-Brunhes event. Geology, 31(3): 239-242.

Watson, A.J. and Naveira Garabato, A.C., 2006. The role of Southern Ocean mixing and upwelling in glacial-interglacial atmospheric CO_2 change. Tellus Series B-Chemical and Physical Meteorology, 58(1): 73-87.

Yoder, J.A., Ackleson, S., Barber, R. and Flamant, P., 1994. A line in the sea. Nature, 371: 689-692.

Zielinski, U. and Gersonde, R., 1997. Diatom distribution in Southern Ocean surface sediments (Atlantic sector): Implications for paleoenvironmental reconstructions. Palaeogeography Palaeoclimatology Palaeoecology, 129(3-4): 213-250.
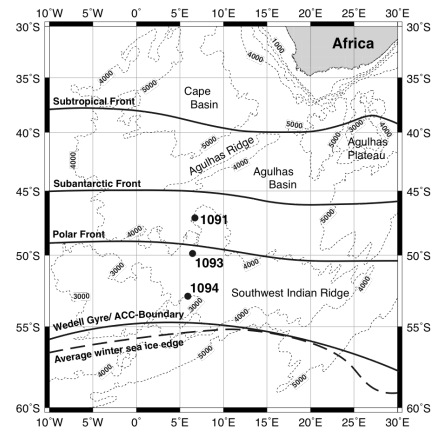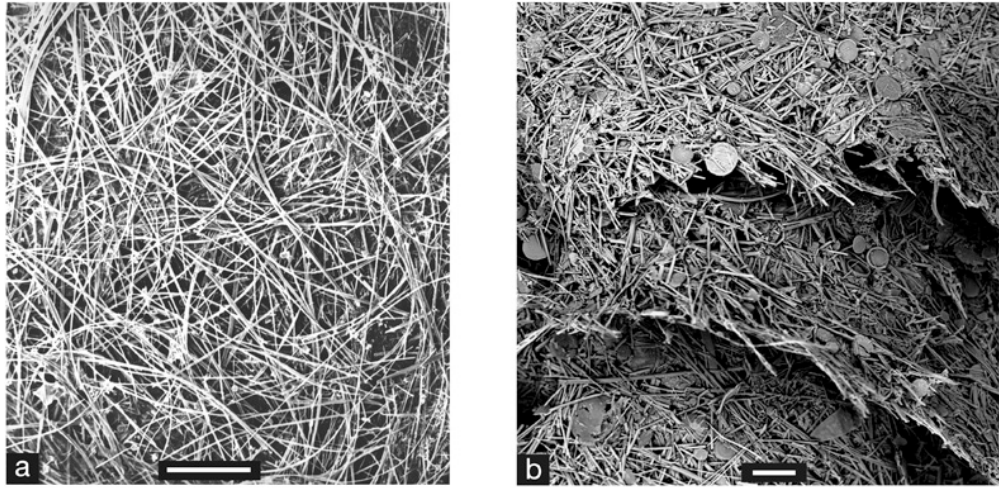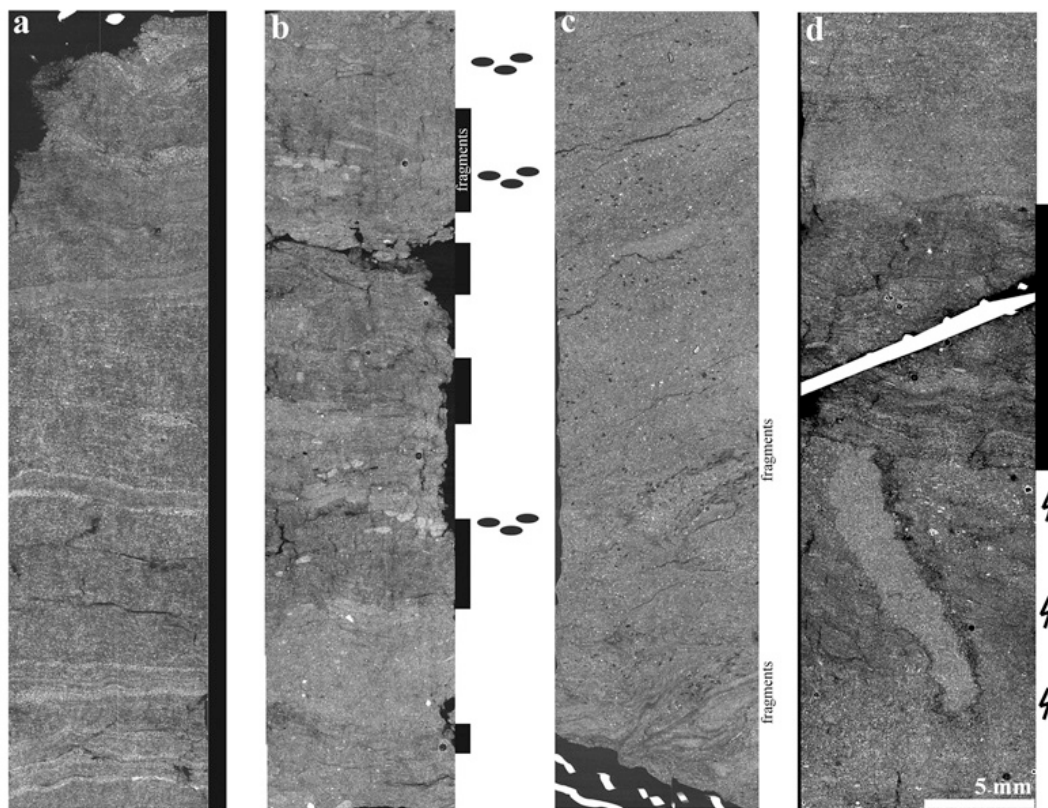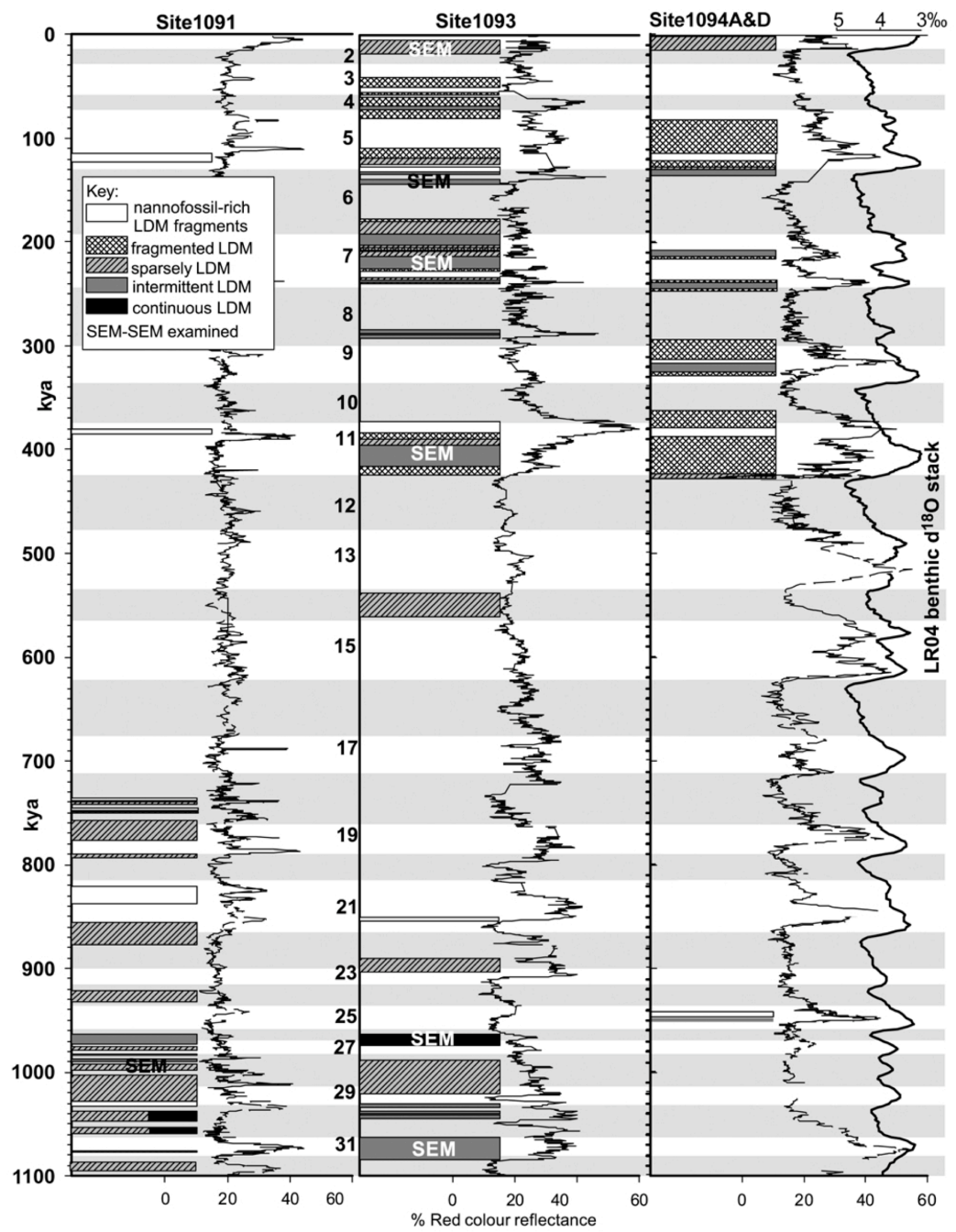
Fig. 1

Figure 2

Figure 3

Figure 4

Fig. 5

a

IRM@AF(A/m)

Step increase in dust input to Mediterranean
due to aridification of North Africa

b 750 ———————— 870 — 890 ——— 920 – 930 – 940 – 955

Second northward
move of Polar front
marked by cessation
of LDMs at Site 1091

Cooling of Benguela
Coastal Current

First northward
move of Polar Front
marked by cessation
of LDMs at Site 1093

Step reduction in
DWBC flow

Onset of low
carbonate in
South Atlantic

Last mid-Pleist.
Sapropel (S″)

870-920

SST minimum in
equatorial oceans and
North Atlantic

c

Insolation (65°N (Wm⁻²)

e 400   e 100
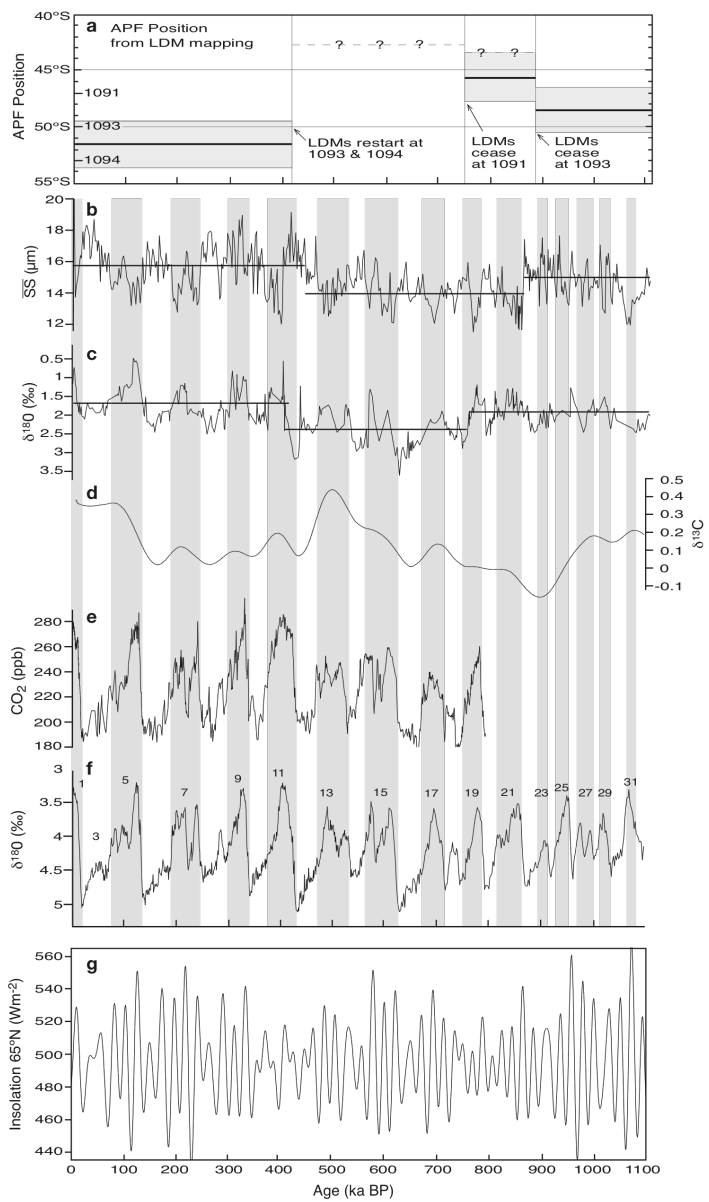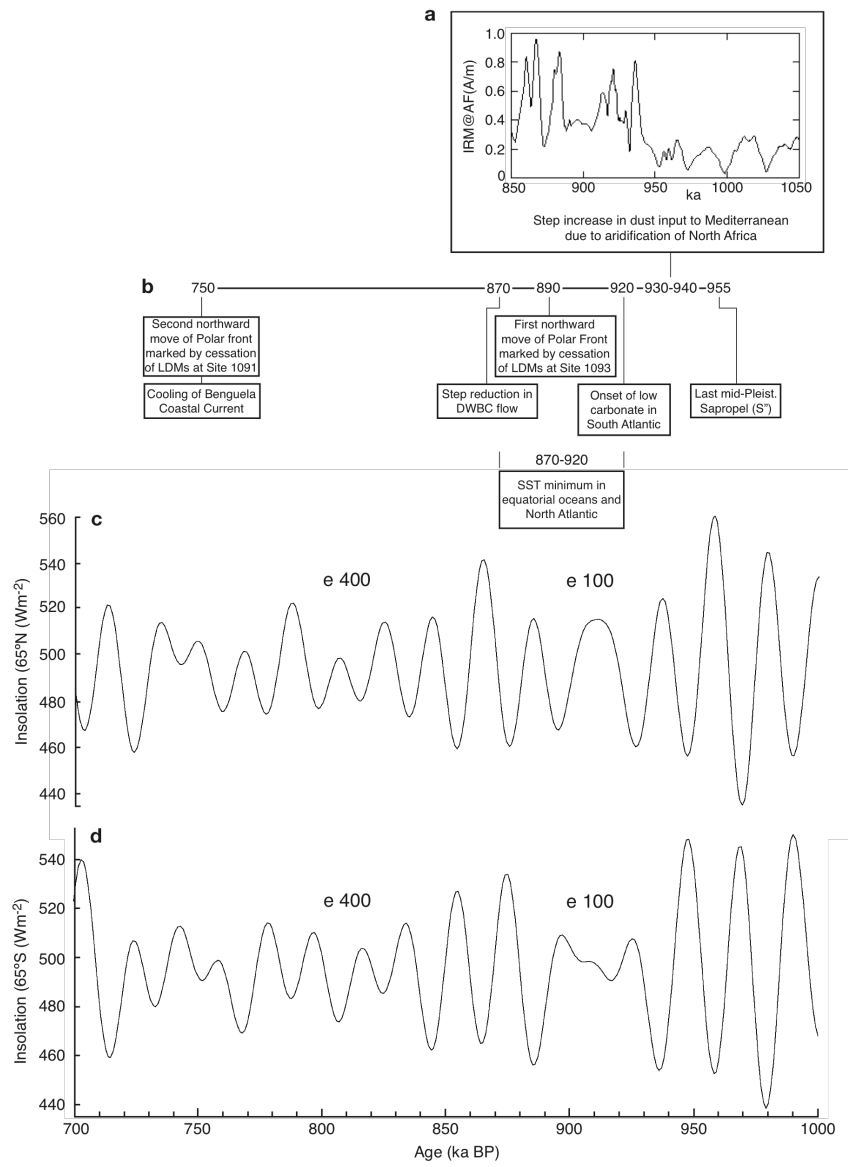
d

Insolation (65°S (Wm⁻²)

e 400   e 100

Age (ka BP)

Fig. 6

Figure 6

54

Fig. 7

Figure 7